INTERNATIONAL ATOMIC ENERGY AGENCY
UNITED NATIONS EDUCATIONAL, SCIENTIFIC AND CULTURAL ORGANIZATION

INTERNATIONAL CENTRE FOR THEORETICAL PHYSICS
34100 TRIESTE (ITALY) - P.O.B. 586 - MIRAMARE - STRADA COSTIERA 11 - TELEPHONES: 224281/2/3/4/5/6
CABLE: CENTRATOM - TELEX 460392 - I

SMR/100 - 15

WINTER COLLEGE ON LASERS, ATOMIC AND MOLECULAR PHYSICS

(24 January - 25 March 1983)

Molecular Spectroscopy with IR Lasers

D. BASSI

Libera Università degli Studi
Dipartimento di Fisica
38100 Trento
Italy

These are preliminary lecture notes, intended only for distribution to participa
Missing or extra copies are available from Room 230.

Davide Bassi

Lectures to be given at the Winter College on lasers, atomic and molecular physics.

International Centre for Theoretical Physics

Trieste 1983.

Summary

Lecture 1 (see papers 1 and 2)

Principles and properties of molecular beam Opto-Thermal Infrared Spectroscopy (O.T.I.S.).

Experimental methods for O.T.I.S.

Currently available tunable infrared lasers.

Thermal detectors

Lecture 2 (see papers 1 and 3)

Application of O.T.I.S. to molecular beam diagnostics and state preparation.

Seminar (see papers 3 and 4)

Sub-doppler spectroscopy of low J transitions of the ν_3 band of sulfur hexafluoride.

Rabi oscillations.

Experimental observation of Ramsey Fringes.

Description of Ramsey Fringes by a 2 x 2 matrix formalism.

Lecture 3 (see paper 5)

Application of O.T.I.S. to multiple-photon infrared absorption.

State resolved rotational relaxation of CO in the free jet expansion of He–CO mixtures

D. Bassi, A. Boschetti, S. Marchetti,[a] G. Scoles,[b] and M. Zen

Unità CNR-GNSM, Dipartimento di Fisica, Universita di Trento, Italy
and Istituto per la Ricerca Scientifica e Tecnologica, 38050 Povo (Trento), Italy

(Received 29 September 1980; accepted 16 October 1980)

We describe an infrared molecular beam spectrometer which uses a semiconductor diode laser and has been used to study the rotational relaxation of CO molecules in the free jet expansion of pure CO and a 90% He–10% CO mixture. The data for the mixture are analyzed by means of a kinematical method based on the use of the master equation and empirically scaled state to state rate constants. Information of the He–CO rotationally inelastic rate constants are obtained. The possibility of using free jet expansion to study rotational inelastic collisions is discussed.

INTRODUCTION

Free jet expansions of pure and mixed gases are the established source for high intensity molecular beams and therefore have been subjected to extensive experimental and theoretical studies.[1,2] Moreover the free jet itself represents an interesting problem that has attracted continuing attention from people interested in aerodynamics and its applications.[3]

The study of the rotational relaxation of a polyatomic molecule in free jets is of interest on two counts. First, one would like, given the source conditions, to be able to predict the populations of individual rotational levels once the expansion is terminated and the molecular beam has been sampled. Second, there is the hope that a better understanding of both, jets and the mechanism of rotational relaxation, may emerge from these studies. For instance, the jet itself represents a unique environment because of the presence, in it, of very low energy collisions which can be duplicated only with great difficulty in equilibrium experiments but are of substantial importance in unusual physical conditions as those prevailing in interstellar gas clouds.[4] Several experimental techniques have been used so far to study rotational relaxation in free jets. The list includes electron beam induced fluorescence,[5] velocity distribution measurements followed by energy balance,[6] impact-pressure measurements,[7] molecular beam laser induced fluorescence,[8] molecular beam maser techniques,[9] Raman spectroscopy,[10] infrared absorption spectroscopy,[11] molecular beam electric and magnetic resonance spectroscopy,[12] and, finally, electrostatic, state selective, beam focusing measurements.[13]

The merits and shortcomings of this plethora of techniques are too numerous to be discussed here in detail. We will, instead, follow the inverse procedure and will list all the qualities that the measuring technique should possess in order to produce useful results. One should be able, in principle, to probe, with good signal to noise ratios and good spatial resolution, as many states as possible, at small and large distances from the nozzle, in a wide range of pressures, for a range of molecules with substantially different moments of inertia. Most of these requirements stem from the fact that several (but not all) of the previous investigators have detected interesting deviations from Boltzmann-like distributions (especially for the sparsely populated high *J* levels) which, in principle, contain considerable information on both rotational relaxation and free jet expansions. In our opinion only molecular beam laser induced fluorescence has most of the qualities indicated above and has indeed provided us with some of the best sets of experimental results.[4] Nevertheless, laser induced fluorescence, in absence of easily available tunable UV lasers, can be applied only to molecules with a visible spectrum, while most bulk relaxation studies and theoretical investigations, on both potentials and inelastic collisions, have been conducted on "simpler" molecules like N_2, CO, HF, H_2, etc.

Recently, substantial progress has been made in the sensitivity and resolution with which infrared spectroscopy can be carried out with molecular beam samples by the use of cw tunable lasers and bolometric detection of the excitation of the molecules in the beam.[14] This technique has also been applied to the study of the rotational relaxation of He–HF mixtures using a color center laser as the source of tunable radiation.[15] During the course of this work Gough and Miller have also developed a kinetic method to model the free jet expansion based on the use of the master equation and empirically scaled state to state rate constants.[15,16]

In the present paper we will describe an infrared molecular beam spectrometer which uses a semiconductor diode lasers and has been used to study the rotational relaxation of CO molecules in the free jet expansion of pure CO and a 90% He–10% CO mixture. The method of Gough and Miller is used to analyze the data (for the mixture only) and, through it, information is obtained on He–CO rotationally inelastic rate constants.

There are several reasons why He–CO mixtures deserve to be singled out for this type of studies: (1) Atom–diatom collisions are much better understood than diatom–diatom collisions and almost exact methods are available for the calculation of inelastic cross sections and their energy dependence.[4] (2) The He–CO

---

[a] Present address: CNEN, Centro di Frascati, Frascati (Roma), Italy.

[b] Permanent address: Chemistry Department, University of Waterloo, Waterloo, Ontario, N21 3G1 Canada.

0021-9606/81/042221-07$01.00

potential has been extensively studied and the sensitivity of the inelastic cross sections to changes in the potential has been checked.[17] (3) He–CO collisions at very low relative energies, as available in the free jet expansion, are of interest for the calculation of cooling rates in interstellar gas clouds.[4] (4) The bulk relaxation of CO and He–CO mixtures has been the subject of several experimental and theoretical papers.[18] (5) Finally, the total differential[19] and the integral[20] scattering cross section for He scattered by CO have been measured while state resolved, rotationally inelastic, differential cross section measurements are underway.[21]

In the next section we will describe the apparatus and experimental procedures while the results will be presented, analyzed and discussed in the third and fourth part of the paper.

EXPERIMENTAL

The experimental setup, shown schematically in Fig. 1, is a modified version of the apparatus of Ref. 14 and consists of a three-chamber molecular beam machine with an IR laser spectrometer set up next to it. In the first chamber, pumped by a 5300 l s^{-1} diffusion pump, we find the supersonic free jet expansion produced through a room temperature x y z movable nozzle N of $40 \pm 3 \times 10^{-4}$ cm diameter. With typical source pressures between 1 and 5 atm the pressure in the first chamber is of the order of 10^{-4} Torr. The molecular beam is sampled, at 1.5 cm downstream from the nozzle, by a conical collimator K with a 4×10^{-2} cm diameter opening on its tip. Through this collimator the beam enters the second chamber where, with a pump of 2000 l s^{-1}, pressures of the order of 2×10^{-7} Torr are normally maintained. In the second chamber the beam can be interrupted with the shutter S, modulated with the chopper C1 and detected with the liquid He cooled, doped Si, bolometer B located at a 40 cm distance from the nozzle. The bolometer's static responsivity is 1.3×10^5 V W^{-1} while its rms noise under operating conditions is about 400 nV · Hz$^{-1/2}$. The bolometer can be rotated away out of the beam path so that the beam molecules may proceed to the third chamber where a quadrupolar mass spectrometer QM is located which measures beam composition and time of flight spectra. The vacuum in this chamber is about 10^{-10} Torr and is obtained by means of a turbomolecular pump TP coupled, by means of a differential arrangement (see Fig. 1), with the chemical getter pump GP. The laser DL is a semiconductor (PbS$_{1-x}$Se$_x$) diode laser from Laser Analytics (now Spectraphysics). The power of the emitted radiation is of the order of 1 mW tunable in a range of about 50 cm^{-1} around the CO centerband. The radiation is emitted within several modes separated by about 1.5 cm^{-1} with normally one mode dominating on the others. The linewidth of each mode was about 20 MHz. The laser beam is focused by a couple of 1 in. diam antireflection coated Ge lenses (L1: $f = 1$, L2: $f = 5$) and is split and chopped by the mirror chopper C2. During half of the time the beam crosses the molecular beam at right angles and is thereafter monitored with the pyroelectric detector D2. During the other half is deflected at right angles by C2 and is sent through a gas cell AC to detector D1 or to the Beckmann (model 4220) IR spectrometer for frequency identification. When the laser light is tuned exactly at the frequency of a transition the internal energy of the molecules in the beam is periodically increased and the bolometer will detect a signal which is proportional to the population of the molecules in the state where the transition starts and to the power present in the laser mode which pumps the transition. The sources of error are basically two. For the high J states, which at high source pressures are sparsely populated, the low signal level is the limiting factor. For the low J states (where signal to noise ratios are in excess of 100) the limiting factor is the precision with which the power present in the pumping mode is measured. To increase this precision another cell D1 (also shown in the figure) containing enough CO (to absorb totally the radiation at resonance) was located between the laser and detector D2. The change in signal level in D2 when the relevant laser mode was absorbed in the cell provided an adequate measure of the quantity in question.

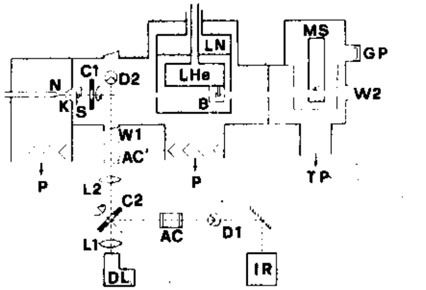

FIG. 1. Schematic view of the apparatus (see text).

RESULTS AND ANALYSIS

The rotational relaxation results relative to the free jet expansion of pure CO and of the 10% CO–90% He mixture are shown in Table I. The $N'(J)$ quantities reported are the populations of the different J levels, relative to the $J = 0$ level, corrected for degeneracy, laser power, and transition dipole strengths. The intensity of a R_J transition is

$$I_J \propto N(J) \, |\mu_{IJ}|^2 \ ,$$

where $N(J)$ is the population of the lower state and μ_{IJ} is the transition dipole matrix element which is proportional to $(J+1)\,(2J+1)^{-1}$.

Neglecting saturation effects, the bolometer signal is given by

$$S(J) \propto N(J)\,(J+1)\,(2J+1)^{-1}\,W(J) \ , \qquad (1)$$

where $W(J)$ is the power of the laser mode pumping the transition. The degeneracy corrected, relative populations are then

$$N'(J) = N(J)\,N(0)^{-1}\,(2J+1)^{-1} \ , \qquad (2)$$

TABLE I. Degeneracy corrected rotational populations $N'(J)$ relative to the $J = 0$ state in molecular beams sampled from free jets of pure CO and 10% CO–90% He mixtures at different stagnation source pressures.

		Pure CO			
J	1.3 atm	2 atm	3 atm	4 atm	5 atm
0	1 ± 10%	1	1	1	1
1	0.57 ± 10%	0.54	0.50	0.43	0.41
2	0.27 ± 15%	0.25	0.19	0.125	0.104
3	0.115 ± 20%	0.078	0.044	0.033	0.025
4	0.025 ± 20%	0.015	0.009	0.0054	0.0039
5	0.0095 ± 25%	0.0044	0.0024	0.0012	0.0008
		10% CO–90% He mixture			
J	1.3 atm	2 atm	3 atm	4 atm	
0	1 ± 10%	1	1	1	
1	0.496 ± 15%	0.398	0.308	0.240	
2	0.188 ± 20%	0.117	0.062	0.037	
3	0.057 ± 25%	0.025	0.0092	0.0055	

or, using Eq. (1),

$$N'(J) = S(J)\,S(0)^{-1}\,W(J)^{-1}\,W(0)\,(J+1)^{-1} \ , \qquad (3)$$

which are the quantities reported in Table I. In an attempt to define a rotational temperature the population data can be plotted in a $\ln N'(J)$ vs $J(J+1)$ type of plot where, in the case the data would follow a straight line, the slope of the line would give the wanted temperature.

Such plots are shown in Fig. 2. In the figure the population data corresponding to different pressures have been multiplied by arbitrary constant factors for sake of clarity. From the plots it is quite apparent that the data do not follow straight lines and that a rotational temperature cannot be defined. We have also measured, with the TOF spectrometer, the velocity distributions of both He and CO in the expanding pure CO and He–CO mixture and the results are reported in Table II. The entries in this table are derived through fits to the experimental TOF distributions assuming that the signal of the density sensitive mass spectrometer is given by $S(v) = v^2 \cdot \exp\{-[\alpha^{-2}(v-u)^2]\}$ where u is the stream velocity, and v the random velocity superimposed to it. This function convoluted with the trapezoidal opening function of the chopper allows for the measurement of the stream velocity u with a precision of about 1% and of the width of the distribution α with an error of 5%. The last column in Table II lists the translational temperatures derived from the TOF data and from the relationship $T_{\parallel} = \alpha^2 m / 2K^4$ where K is Boltzmann's constant and m is the mass of the corresponding atom (or molecule). We have also measured the velocity distribution of a jet of pure He (actually the stream velocity of beams from high pressure He jets did serve as a calibration for all other velocity measurements). From a comparison of the pure He data with the He data of the mixture we have concluded that the asymptotic terminal velocity spread was, in the latter case, about 15% larger than in the former.

From Table II it is apparent that the jets of pure CO generate measurable quantities of CO dimers which have a small velocity slip with respect to the monomer but essentially the same translational temperature. Dimers were also present, in large relative quantities and equivalent absolute quantities, in the CO seeded beams. The data analyzed were data for which the dimer mass spectrometer signal was no more than 1% of the monomer signal which excludes all data taken at stagnation pressures greater than 2280 Torr (3 atm). Since a large fraction of the dimers is fragmented in the mass spectrometer ion source the 1% limit imposed above provides us only with a lower limit to the actual

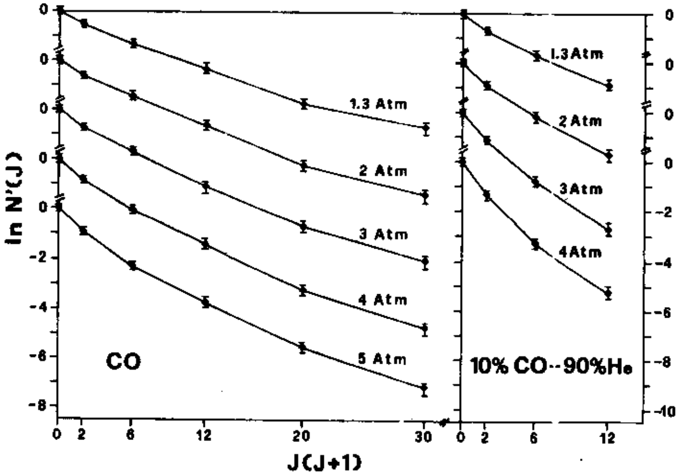

FIG. 2. Experimental rotational state populations (relative to the $J = 0$ level) of CO sampled from the free jet expansion of pure CO and 10% He mixtures. The results obtained for different stagnation source pressures are linked by solid lines and are shown shifted on the vertical scale for sake of clarity.

TABLE II. Velocity distributions of molecular beams sampled from free expanding jets at different stagnation source pressures.

P (Torr)	u (m s^{-1})	α (m s^{-1})	T (K)
CO from the expansion of pure CO			
990	759 ± 1%	87 ± 5%	12 ± 10%
1520	761	81	11
2280	764	76	10
3040	766	71	8.5
3800	770	64	7
4560	773	59	5.8
5320	773	55	5.2
6080	772	54	5
6840	772	54	5
(CO)$_2$ from the expansion of pure CO			
3800	733	38	5
5320	740	38	5
6840	747	38	5
CO from the expansion of the He–CO mixture			
280	1090	186	59
400	1192	153	40
560	1270	137	32
670	1310	118	23
950	1344	91	14
1140	1366	79	10
1520	1405	66	7.3
2280	1411	58	5.7
3040	1425	55	5.1
3800	1426	50	4.2
4560	1430	50	4.3
5320	1433	46	3.6
6080	1433	45	3.5
He from the expansion of the He–CO mixture			
280	1158	330	26
400	1229	272	18
560	1313	252	15
670	1350	210	11
950	1385	174	7.3
1140	1390	162	6.3
1520	1434	150	5.4
2280	1482	120	3.5
3040	1487	106	2.7
3800	1489	98	2.3
4560	1492	91	2
5320	1493	86	1.8
6080	1494	84	1.7

dimer concentration in the beam. The actual concentration of (CO)$_2$ in the beam when the dimer/monomer ratio in the mass spectrometer is 1% could be as high as 5%. In order to analyze rotational relaxation data obtained from beam sampling of free jet expansion several methods have been followed in the past which differ widely in complication and accuracy. These methods can be divided basically into two categories. In the first we find those which postulate the existance of a rotational temperature T_R[22,6(b)–6(d)] which may be frozen at values far from those required by equilibrium with the translational temperature but always leads to Boltzmann-like state distributions. In the second category we find the methods that combine a thermodynamic modelling of the expansion with a kinetic description of the relaxation that makes use of the master equation and of state to state rate constant.[6(a),23] To the second category belongs the method of Gough and Miller,[15,16] which, in a way quite similar to that of Ref. 23(a), allows for the calculation of the population of individual levels. The resulting distribution does not need to, and in general does not, follow a Boltzmann-type statistical distribution. Therefore in agreement with Refs. 23(a), 15, and 16 we (a) model the expansion using the results of Ashkenas and Sherman[24] (adopting, of course, for γ the value appropriate to our mixture, i.e., 1.64), (b) use the master equation to calculate the population evolution of the individual rotational levels, and (c) use numerical integration to obtain the terminal rotational distribution starting at a point $\bar{X}$ in the expansion where it is reasonable to assume that the rotational and translational temperatures are still in mutual equilibrium. Of course, we choose to work with $\bar{X}$ values as large as possible in order to save computer time. Stability of the results with respect to the choice of $\bar{X}$ has been found to be excellent. The value of $\bar{X}$ adopted in all calculation was equal to one nozzle diameter. If $n(J)$ is the population in level J at $\bar{X}$ and k_{KJ} the rate constants for rotational relaxation, we have

$$n'(J)=n(J)+n\,\Delta t\left\{\sum_{K\neq J}\left[k_{KJ}\,n(K)-k_{JK}\,n(J)\right]\right\}\quad, \qquad (5)$$

which can be used to calculate the new distribution at a small time Δt later. During this time the stream velocity will carry a representative sample downstream so that the next calculation will be performed at a slightly larger $\bar{X}$ and hence at a lower $T_{\parallel}$. Iteration until terminal conditions will produce the terminal distribution over the rotational states. Stability of the results, with respect to the length of the elementary step size Δt, and the way in which terminal translational conditions are determined, has also been thoroughly checked. The terminal *rotational* distribution depends sensitivity on the temperature profile along the jet center line in the initial and intermediate region only, while what happens in the final stages of the expansion is relevant merely to the translational properties of the jet because collisions there are just a few and are, therefore, not sufficient to alter appreciably the rotational distribution.

To determine translational terminal conditions we have used the results of Refs. 25 and 26. Typically for stagnation conditions $T=300$ K, $P=2$ atm the terminal width of the He velocity distribution calculated by our program is 138 m s^{-1} to be compared with 150 m s^{-1} as derived from Table II. We could, without appreciably affecting the distribution over the rotational states, bring the above-quoted numbers in exact coincidence by changing the input value for the effective atomic diameter (i.e., changing the mean free path at the nozzle), but this would serve no useful purpose, and would also be unjustified without taking into account all the complication due to the fact that the expanding gas is a (albeit dilute) mixture.[6(d)] Therefore we have chosen an effective He diameter of 2.7 Å^3 and, after verification that our results did not critically depend on this choice,

---

we have kept this value constant throughout our calculations.

Finally, in agreement with the majority of the previous papers dealing with free jets (see, for example, Ref. 3), we have not used in the calculations the measured nozzle diameter, but an "effective" nozzle diameter which is 12% smaller[3] than the nominal one.

DISCUSSION

With respect to the rate constants for the inelastic transitions we have used those calculated by Green and Chapman (GC),[18(a)] extrapolating the rates missing in their tables by making use of the inverse power scaling law $\ln[k_{JK}(2K+1)^{-1}]=\ln k_0+\ln(\Delta E^{-n})$, introduced recently by Pritchard and co-workers.[27] Since GC carried out their calculations at a finite set of temperatures between 10 and 100 K, we have interpolated the other needed values by means of quadratic fits to the values of the power low parameters k_0 and n obtained at the available temperatures. For even ΔJ we have found $k_0=\exp(18.9773 - 0.0391\,T+2\times10^{-4}\,T^2)$ and $n=1.9463-13.54\times10^{-3}\,T + 8.42\times10^{-5}\,T^2$. For the odd ΔJ transitions $k_0 =\exp(15.1161-6.5\times10^{-3}\,T+2.9\times10^{-5}\,T^2)$ and $n=1.06 -6.9\times10^{-3}\,T+3.8\times10^{-5}\,T^2$. No data above 100 K are needed because the detailed calculation of the population in the jet always started (see previous section) when the temperature was below this value. The results obtained with 2 atm in the source, using the GC rate constants are shown as curve a in Fig. 3. The predicted populations appear to be in good agreement with experiment and the deviations from the Boltzmann distributions are clearly reproduced. Until this point, from the point of view of the rate constant, we have considered the 10% CO in He mixture as a infinitely dilute mixture considering identical the probabilities for inelastic transitions in CO–CO and CO–He collisions. This is clearly wrong and a correction is called for. Unfortunately inelastic rate constants for CO–CO collisions are not available in the literature and one has to resort to estimates based on sound absorption[28] or Senftleben–Beenakker effect[29] measurements. Using sound absorption measurements[28] one can see that for both O$_2$–He and N$_2$–He mixtures He–molecule collisions are about as effective as molecule–molecule collisions in relaxing rotational energy. Data on He–CO mixtures are missing but since CO–CO collisions are somewhat more effective than N$_2$–N$_2$ collisions[18(c)] we can conclude, from this point of view, that the He–CO rotational relaxation rates are in average a maximum of two times as small as the corresponding CO–CO rates. On the other hand it is well known, from molecular beam scattering differential cross section measurements,[30,31] that the nonsphericity of the N$_2$–N$_2$ potential affects the scattering pattern[30] (in the form of quenching the rainbow oscillation) while this is hardly the case for the diffraction oscillations present in He–N$_2$ collisions.[31] Although this could be a purely elastic effect it, nevertheless, seems to indicate that the factor of 2 ratio discussed above may indeed be too small. Considerations based on ratios between cross sections relevant to Senftleben–Beenakker measurements[29] coupled to data on the viscomagnetic effect on pure diatomic gases[32] and their mixtures with noble gases[33] suggest that rotation relaxes seven times faster in pure N$_2$ as in N$_2$–He mixtures. This value seems quite high and will be taken as an upper limit for our correction which concerns He–CO mixtures.

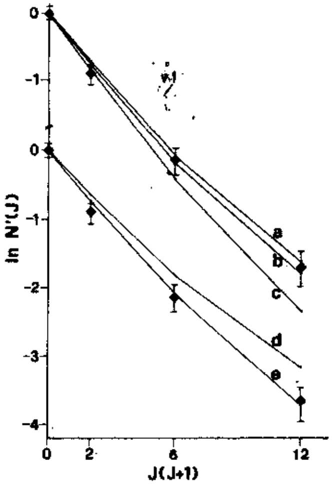

FIG. 3. Comparison between experimental and calculated rotational state populations (relative to the $J=0$ level) of CO sampled from the free jet expansion of a 10% CO–90% He mixture with stagnation pressure of 2 atm. The experimental points (♦) refer to the same experimental conditions, but are shown shifted on the vertical scale to avoid overlap between calculated lines. Solid line *a*: Green and Chapman rate constants, no CO–CO/CO–He correction. Line *b*: GC rate constants, correction factor = 2. Line *c*: GC rate constants, correction factor = 7. Line *d*: Thomas *et al.*[34] rate constants, correction factors = 2. Line *e*: Thomas *et al.*[34] rate constants, correction factor = 7.

We have then recalculated the rotational distributions with the correction included and the results are shown in Fig. 3 as curve b and c (CO–CO rates equal to 2 and 7 times the CO–He rates, respectively). The agreement with experiment is of course worsened, the population of the $J=3$ level (relative to the $J=0$ population) being about a factor of 2 smaller than the measured one.

Nevertheless it should be noted that the first few cross sections pertinent to rotational energy change in He–CO collisions have been recalculated recently by Thomas, Kraemer, and Dierksen[34] starting from an interaction potential calculated using a configuration interaction algorithm which is, by a substantial amount, more reliable (and also more expensive) than the electron gas model used by Green and Thaddeus in their calculation of this interaction.[4] Unfortunately the cross sections calculated in Ref. 34 are just a few and they have not been integrated to yield rate constants. Nevertheless the comparison between the results of Refs. 4 and 34 carried out in the latter paper reveals systematic deviations with all odd cross sections being 30% larger and all

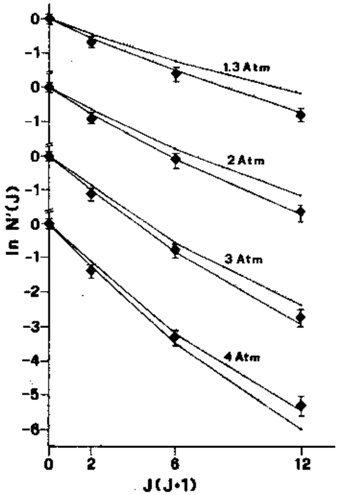

FIG. 4. Comparison between experimental and calculated rotational state populations (relative to the $J = 0$ level) of CO sampled from the free jet expansion of a 10% CO–90% He mixture at several values of the stagnation pressure. ♦ Experimental points. Upper and lower solid lines are calculated with the rate constants of Thomas *et al.*[34] and the CO–CO/CO–He correction factor equal to 2 and 7, respectively.

even cross sections 140% smaller in the second paper with respect to the first. Moreover this difference is not a strong function of the energy of the collision if one excludes the very low energies where due to the presence of resonances, an accurate comparison is difficult anyhow. In view of the above we have considered useful to recalculate our distributions over the states, transferring to all rate constants the corrections which are valid for the first four cross sections of the collision matrix. The results are shown in Fig. 3 as curves d and e (corresponding to the two extreme values of the correcting factor that allows for CO–CO collisions). The agreement with experiment remains substantially unchanged although the best results are now obtained for a correcting factor equal to 7 while before the best value was 2. In Fig. 4 we compare experimental distributions over states with those calculated using the rate constants of Ref. 34 at all pressures for which condensation free data have been obtained. The agreement between experiment and theory is satisfactory but in view of the many approximations and corrections involved in the calculations and the experimental uncertainties (both random and systematic) we feel that more diluted He–CO mixtures should be measured (our attempts in this direction have been thwarted by the premature death of our diode laser) and similar data should be obtained for other monatomic–diatomic gas combinations for which good potentials and rate constants can be or have been calculated (He–H_2CO, He–CO_2 among others) before the conclusion is drawn that free jet expansions can be systematically used to obtain detailed and reliable information at low energy rotationally inelastic collisions. However, we believe that it has been shown here that, in the case examined, there is a good match between theoretical and experimental uncertainties and that it would be worthwhile to go a few steps forward in both directions because there is good information to be gained without having to recur to difficult crossed beam experiments. This is the more true the lower is the collision energy considered, because it is quite possible that, for instance, in measurements with high expansion ratios of light–heavy mass mixtures, the contribution to the total relaxation of resonant scattering could be measured. To this end a dilute parahydrogen CO_2 mixture appears to be one of the most promising candidates.

ACKNOWLEDGMENTS

It is a pleasure to thank Dr. R. Penco for his contributions to the design and the construction of the facility in which this experiment has been carried out, Dr. A. Valentini for his help with the mass spectrometric measurements, and Dr. R. Miller for his help in the analysis of the data. Thanks are also due to Dr. T. E. Gough, Dr. F. R. McCourt, and Dr. J. B. Fenn for very useful discussions. It is finally our pleasure to acknowledge the friendly and expert cooperation of the technical staff of the Physics Department at Trento.

[1] J. B. Anderson, R. P. Andres, and J. B. Fenn, Adv. At. Mol. Phys. 1, 345 (1965).

[2] J. B. Anderson, R. P. Andres, and J. B. Fenn, Adv. Chem. Phys. 10, 275 (1966).

[3] R. Cattolica, F. Robben, L. Talbot, and D. R. Willis, Phys. Fluids 17, 1793 (1974).

[4] S. Green and P. Thaddeus, Astrophys. J. 205, 766 (1976).

[5] (a) E. P. Muntz, Phys. Fluids 5, 80 (1962); (b) P. V. Marrone, *ibid.* 10, 521 (1967); (c) H. Ashkenas, *ibid.* 10, 2509 (1967); (d) P. B. Scott and T. Mincer, Entropie 30, 170 (1969); (e) D. Coe, F. Robben, L. Talbot, and R. Cattolica, Rarefied Gas Dyn. Proc. Int. Symp. 11, 907 (1979); (f) B. N. Borzenko, N. V. Karelov, A. K. Rebrov, and R. G. Sharafutdinov, J. Appl. Mech. Tech. Phys. 17, 615 (1977).

[6] (a) D. R. Miller and R. P. Andres, J. Chem. Phys. 46, 3418 (1967); (b) R. J. Gallagher and J. B. Fenn, *ibid.* 60, 3487 (1973); (c) 60, 3492 (1973); (d) P. Poulsen and D. R. Miller, Prog. Astronaut. Aeronaut. 51, 899 (1977); (e) U. Buck, H. Pauly, D. Pust, and J. Schleusener, Rarefied Gas Dyn. Proc. Int. Symp. 9, C10 (1974); (f) K. Winkelman, Rarefied Gas Dyn. Proc. Int. Symp. 11, 899 (1979); (g) S. Yamazaki, M. Taki, and Y. Fujitani, private communication (1980).

[7] B. Lefkowitz and E. L. Knuth, in *Related Gas Dynamics*, edited by L. Trilling and H. Y. Wachman (Academic, New York, 1969), 1421.

[8] (a) M. P. Sinha, A. Schultz, and R. N. Zare, J. Chem. Phys. 58, 549 (1973); (b) K. Bergmann, W. Demtröder, and P. Hoving, Appl. Phys. 8, 65 (1975); (c) R. E. Smalley, B. L. Ramakrishna, D. H. Levy, and L. Wharton, J. Chem. Phys. 61, 4363 (1974); (d) R. E. Smalley, L. Wharton, and D. H. Levy, J. Chem. Phys. 63, 4977 (1975); (e) R. E. Smalley, D. H. Levy, and L. Wharton, J. Chem. Phys. 64, 3266 (1976); (f) P. J. Dagdigian, J. Chem. Phys. 64, 2609 (1976); (g) C. Y. R. Wu, J. B. Gooke, S. C. Yang, K. R. Way, and W. C. Stwalley, Rev. Sci. Instr. 49, 380 (1978).

[9] S. G. Kukolich, D. E. Oates, and J. H. S. Wang, J. Chem. Phys. 61, 4686 (1974).

[10] (a) I. F. Silvera and F. Tommasini, Phys. Rev. Lett. 37,

136 (1976); (b) I. F. Silvera, F. Tommasini, and R. J. Wij-Wijngaarden, Prog. Astronaut. Aeronaut. 51, 1295 (1977).

[11] D. N. Travis, J. C. McGurk, D. McKeown, and R. G. Denning, Chem. Phys. Lett. 45, 287 (1977).

[12] (a) T. R. Dyke, G. R. Tomasevich, W. Klemperes, and W. E. Falconer, J. Chem. Phys. 57, 2277 (1972); (b) W. L. Meerts, G. ter Horst, J. M. L. J. Reinartz, and A. Dymanus, Chem. Phys. 35, 253 (1978); (c) J. Verberne, I. Ozier, L. Zandee, and J. Reuss, Mol. Phys. 35, 1649 (1978).

[13] (a) V. Borkenhagen, H. Malthan, and J. P. Toennies, J. Chem. Phys. 63, 3173 (1975).

[14] T. E. Gough, R. E. Miller, and G. Scoles, Appl. Phys. Lett. 30, 338 (1977).

[15] R. E. Miller, Thesis, University of Waterloo, Waterloo, Ontario, Canada, 1980 (unpublished).

[16] T. E. Gough and R. E. Miller (to be published).

[17] L. D. Thomas, W. P. Kraemer, and G. H. F. Diercksen (to be published).

[18] (a) A. P. Malinauskas, J. W. Gooch, Jr., B. K. Annis, and R. E. Fuson, J. Chem. Phys. 53, 1317 (1970); (b) I. Amdur and L. M. Shuler, J. Chem. Phys. 38, 188 (1963); (c) P. G. Kistemaker, A. Tom, A. E. de Vries, Physica (Utrecht) 48, 414 (1970); (d) G. J. Prangsma, A. H. Alberga, and J. J. M. Beenakker, *ibid.* 64, 278 (1973); (e) R. Goldflam, D. J. Kouri, and S. Green, J. Chem. Phys. 67, 5661 (1977); (f) A. E. DePristo and H. Rabitz, J. Chem. Phys. 68, 1981 (1978); (g) S. Green and S. Chapman, Astrophys. J. Suppl. Ser. 37, 169 (1978); (h) A. E. DePristo and H. Rabitz, J. Chem. Phys. 69, 902 (1978); (i) J. Quant. Spectrosc. Radiat. Transfer 22, 65 (1979).

[19] M. Keil, J. T. Slankas, and A. Kuppermann, J. Chem. Phys. 70, 541 (1979).

[20] H. P. Butz, R. Feltgen, H. Pauly, and H. Vehmeyer, Z. Phys. 247, 70 (1971).

[21] M. Faubel, K. H. Kohl, and J. P. Toennies (private communication).

[22] (a) C. G. M. Quah, J. B. Fenn, and D. R. Miller, Rarefied Gas Dyn. Int. Symp. Proc. 11, 885 (1979); (b) C. G. M. Quah, Chem. Phys. Lett. 63, 141 (1979).

[23] (a) H. Rabitz and S. H. Lam, J. Chem. Phys. 63, 3532 (1975); (b) K. Koura, Rarefied Gas Dyn. Int. Symp. Proc. 11, 833 (1979).

[24] H. Ashkenas and F. S. Sherman, in *Rarefied Gas Dynamics*, edited by J. H. de Leeuw (Academic, New York, 1966), Vol. 2, p. 84.

[25] J. B. Anderson and J. B. Fenn, Phys. Fluids 8, 780 (1965).

[26] J. B. Anderson, AIAA J. 10, 112 (1972).

[27] D. E. Pritchard, N. Smith, R. D. Driver, and T. A. Brunner J. Chem. Phys. 70, 2115 (1979).

[28] R. Holmes, G. R. Jones, N. Pusat, and W. Tempest, Trans. Faraday Soc. 58, 2342 (1962).

[29] G. J. Prangsma, A. L. J. Burgmans, H. F. P. Knaap, and J. J. M. Beenakker, Physica (Utrecht) 65, 579 (1973).

[30] M. Cavallini, M. G. Dondi, G. Scoles, and U. Valbusa, Chem. Phys. Lett. 10, 22 (1971).

[31] M. Keil, J. T. Slankas, and A. Kuppermann, J. Chem. Phys. 70, 541 (1979).

[32] A. L. J. Burgmans, P. G. van Ditzhuyzen, H. F. P. Knaap, and J. J. M. Beenakker, Z. Naturforsch. Teil A 28, 835 (1973).

[33] A. L. J. Burgmans, P. G. van Ditzhuyzen, and H. F. P. Knaap, Z. Naturforsch. Teil A 28, 849 (1973).

[34] L. D. Thomas, W. P. Kraemer, and G. H. F. Diercksen, Lawrence Berkeley Laboratory, Preprint 10635, 1980.

Applied Physics

Molecular Beam Diagnostics by Means of Fast Superconducting Bolometer and Pulsed Infrared Laser

D. Bassi, A. Boschetti, M. Scotoni, and M. Zen

Istituto per la Ricerca Scientifica e Tecnologica and Unità CNR-GNSM, Dipartimento di Fisica, Università di Trento, I-38050 Povo (Trento), Italy

Received 4 March 1981/Accepted 29 May 1981

Abstract. The laser-bolometric infrared spectroscopy is an efficient method for measuring the internal energy distributions of molecular beams. Additional informations about the kinetic energy distribution of molecules in a selected internal state can be obtained from time resolved experiments. A fast superconducting bolometer and a pulsed infrared CO_2 laser have been used for testing the use of this technique as a universal tool for molecular beam diagnostics. Experimental results are presented and analyzed for pure SF_6 and helium seeded with 5% SF_6 beams. The efficiency of fast superconducting bolometers, used for molecular beam time-of-flight measurements, is discussed. A comparison is made between time resolved laser-bolometric technique and alternative molecular beam diagnostic methods.

PACS: 34.50L, 33.20E, 35.80

Molecular beam collision experiments are a primary source of information about inelastic and reactive molecular interactions in the thermal energy range [1]. A complete characterization of these phenomena requires a knowledge of detailed energy balance, with the contribution of kinetic and internal energy distributions. A chemical analysis is also needed when reactive collisions take place. The measurement of all these quantities, in a single experiment, is a very difficult task and it is possible to restrict the investigation to a limited set of parameters only in a few cases. The experimentation of new, efficient and versatile molecular beam detectors would be of great help in the development of this field. Among the detectors available now, the most popular is the electron bombardment ionizer, followed by a mass spectrometer (usually an electric quadrupole). The principle of operation and the main characteristics of this detector are well known [2]: it is mass selective and is fast enough to measure the kinetic energy distribution of the beam by means of the time-of-flight [3] (T.O.F.) technique. Unfortunately, ionizing detectors cannot be used to analyze internal energy distributions: a dependence of the ionization efficiency from the vibrational state of molecules has been observed, but is not selective enough to allow a quantitative analysis [4]. When mass selection is not needed, cryogenic bolometers are an efficient alternative to ionization detectors [5]. A bolometer works like a microcalorimeter converting the energy released by the beam on its surface to a resistance change. Commercially available bolometers are based on semiconductor crystals (doped silicon or germanium) and have been developed primarily for infrared radiation detection. The typical response time of semiconductor bolometers is in the millisecond range and is too long to perform T.O.F. measurements. A significant improvement in the molecular beam bolometer has been achieved by Gallinaro and coworkers [6, 7], using a thin film of superconducting material as a sensitive element. Their detector reaches a response time around 10^{-6} s, with a noise equivalent power in the 10^{-12} W Hz$^{-1/2}$ range. Cryogenic bolometers can be used to analyze internal energy distributions by means of the so called laser-bolometric technique, introduced in 1977 by Gough et al. [8a]. It consists of measuring the energy absorbed by a molecular beam from a cw tunable infrared laser, as a function of the laser frequency. The absorbed energy is carried by the molecular beam on the surface of a bolometric detector. Radiative losses on the beam path are negligible because infrared decay times are typically longer than molecular flight times. A bolometric signal is observed whenever the infrared laser is tuned on a molecular ro-vibrational transition. This signal is proportional to the concentration of molecules occupying the state involved in the transition.

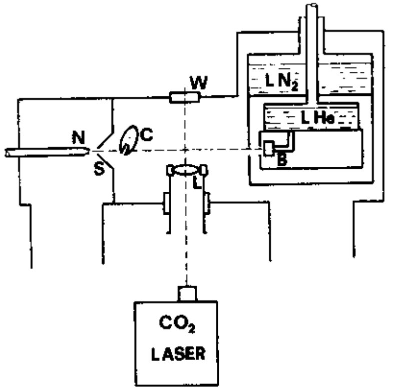

Fig. 1. Experimental set-up (N: supersonic nozzle source; S: skimmer; C: mechanical chopper; L: NaCl lens; B: fast superconducting bolometer; W: optical window)

The laser bolometric technique has been applied, up to now, to several different measurements including sub-doppler infrared spectroscopy [8b, 10], vibrational predissociation of van der Waals molecules [8c, 10] and rotational distribution analysis [9, 10]. In most of these experiments the bolometer is coupled to a mass spectrometer for obtaining, respectively, information about internal states and kinetic energy distributions (T.O.F.). We note that this choice leads to complex experimental apparatus, with multiple differentially pumped vacuum stages, where the main feature of mass spectrometers (i.e. the mass discrimination) may be unnecessary. Indeed the bolometer, when coupled to a tunable infrared laser, becomes by itself a selective device for chemical species [8a]. Starting from this consideration we decided to use the fast superconducting bolometer developed by Gallinaro and coworkers to extend the laser bolometric technique to kinetic energy analysis, by means of pulsed laser sources. Our aim was to demonstrate that time resolved laser-bolometric spectroscopy can be used like a universal tool for molecular beam diagnostics.

Experimental Set-Up and Results

The experimental set-up (shown schematically in Fig. 1) is a modified version of the apparatus described in [9], to which the reader is referred for a detailed description. The present configuration has been arranged for studying the multiphoton absorption and dissociation of SF_6 molecules. Nevertheless this paper will be devoted only to the description and characterization of the bolometric detection system.

The molecular beam is produced by means of a conventional supersonic nozzle source (nominal diameter: 30 µm) and is skimmed before entering the detector chamber. The apparatus can be operated with two different methods for modulating the beam: a) a mechanical chopper, placed 41.5 cm away from the detector, which operates up to a frequency of 450 Hz with a duty cycle 1 to 80; b) irradiating the beam with a pulsed laser when the rotating chopper is stopped in the open position. The light source is a tunable pulsed CO_2 laser (Lumonics TEA 820) which produces infrared radiation with an energy up to 3 J pulses at a maximum rate of 20 Hz. The pulse duration is about 10^{-6} s but the main part of the energy is released during a time interval of about $2 \cdot 10^{-7}$ s. The laser beam is focused on the molecular beam by means of a movable NaCl lens which is used to vary the irradiation conditions. The distance from the lens axis to the detector is 33.5 cm. The superconducting bolometer is made by evaporating a thin film of tin (dimensions 1.7×7 mm^2) on a Al_2O_3 substrate, following the procedure illustrated in [5 and 6]. The film has a room temperature resistance of 20 Ω. When operated around the middle of the superconducting transition temperature (about 3.7 K) the bolometer has a voltage responsivity of 150 V W^{-1}, a noise equivalent power of $5 \cdot 10^{-12}$ W Hz$^{-1/2}$ and a response time of about 10^{-6} s electronically measured. The electronic circuit used for signal detection is shown in Fig. 2. The bolometer is fed by an ultra-stable current source (set at 200 µA) and the signal produced by the resistance change of the bolometer is amplified (× 100) by means of a wideband transformer (Geoformer G.4). A general purpose differential preamplifier (Tektronix AM 502) is used to increase further the signal level before averaging.

The bolometer holder is made of copper and is in poor thermal contact with the bottom of a liquid helium cryostate. A suitable system of copper shields is used to reduce the infrared background radiation. The liquid helium bath is pumped below the He λ-point (to about 1.7 K) to increase its temperature stability. The low frequency component of the bolometric signal is used as a measurement of the holder temperature. A feed back system between this temperature reading and a heater, wound around the holder, is used to provide the temperature stabilization needed for operating the bolometer.

An example of experimental data is presented in Fig. 3. The upper curve (Fig. 3a) corresponds to a time-of-flight spectrum, taken in the usual way by means of mechanical chopper modulation. Figure 3b shows the T.O.F. spectrum of the same molecular beam, obtained by pulsed laser irradiation [P(20) line]. In this second case a continuous beam impinges on the bolometer and a fraction of it is irradiated by a short laser pulse. The bunch of irradiated molecules has an initial length of about 0.5 cm. The energy absorbed by the molecules is carried to the bolometer, after a time depending on the velocity distribution. We assume that the change of internal energy, induced by laser irradiation, has no effect on the velocity distribution of molecules. Indeed the momentum transfer due to photon absorption is negligible and the $V-T$ relaxation cannot take place in the collision free regime of our molecular beam. Our conditions are completely different from those described in a recent paper by Bernstein and coworkers [12]. They have observed the change in the velocity distribution induced by laser irradiation near to the nozzle region, where the density is high enough to allow $V-T$ relaxation. Data in Fig. 3 corresponds, in principle, to two different physical conditions: Fig. 3a gives the T.O.F. spectrum of all the molecules while Fig. 3b give the T.O.F. spectrum for those molecules absorbing the laser line. This measurement could be repeated at different wavelengths to analyze, in details, the velocity distribution of molecules in different internal states. A suitable choice of excitation frequencies can lead to a complete characterization of the beam properties. Figure 3b shows also the presence of a peak at a time near to zero, due to detection of diffused laser radiation. The width of this signal is much longer than the bolometer response time and is actually limited by the transformer band pass. It could be drastically reduced by means of suitable collimators and by blackening the surfaces of the vacuum chamber. Nevertheless, it is a good practice to detect a small fraction of laser light to have a simple and efficient reference for the time scale.

Discussion

Time-of-flight experimental data have been analyzed assuming a velocity distribution given by [2]

$$f(v) \propto v^3 \exp\{-[(v/u)/\alpha]^2\}, \tag{1}$$

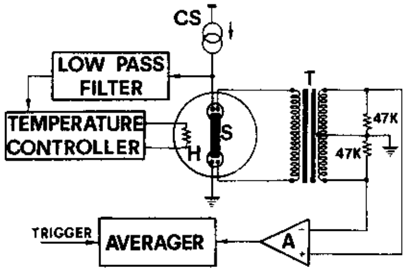

Fig. 2. Electronic circuit for signal detection (CS: current source; H: heating element for temperature stabilization; S: sensitive surface of the bolometer; T: wideband transformer; A: differential preamplifier). The signal to trigger the averager is taken by a lamp-photodiode system from the mechanical chopper or, alternatively, from the laser trigger

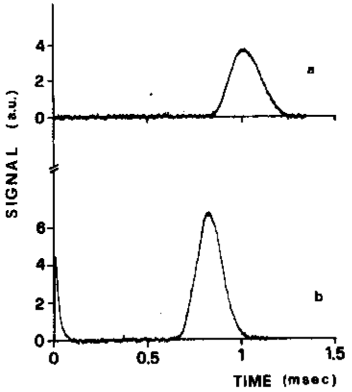

Fig. 3a and b. Experimental time-of-flight spectra of SF_6 (source stagnation pressure 12 bar) taken by a mechanical chopper (a) and by a pulsed CO_2 laser (b). The flight paths are respectively 41.5 and 33.5 cm

where the two parameters u and α are related respectively to the mean flow velocity and to the velocity spread. Equation (1) has been convoluted with the gate function [3] of the mechanical chopper to fit data shown in Fig. 4a, while for optical modulation data no correction is needed because the dimension of the laser spot is negligible compared to the distance between the lens axis and the bolometer. A further convolution would be needed to analyze T.O.F. spectra obtained by means of ionizing detectors, to take into account the distribution of arrival times which are related to the extension of the ionization region. This is not the case for bolometric detectors, because all molecules are detected at the same distance from the starting point (as far as the bolometer surface is placed perpendicularly to the molecular beam axis). A few examples of calculated time-of-flight spectra are shown in Fig. 4 by full lines, superimposed on the corresponding experimental data. A résumé of experimental conditions and best fit parameters for each curve is reported in the figure caption. We remark that data for pure SF_6 beams are probably affected by a systematic error due to the presence of dimers and higher order clusters in the molecular beam. These species have a velocity distribution which may be slightly different from the monomer. We note that the same problem is present also with other detectors like the ionization one, where cluster fragmentation can affect pure monomer measurement. The best fit parameters obtained from pure SF_6 measurements have to be considered like average values and a more accurate study at different wavelengths and laser fluence is needed to obtain more detailed information. The curve in Fig. 4d corresponds to a helium beam seeded with 5% SF_6 at a source pressure of 1.5 bar. In this condition the dimer contribution to the bolometric signal is negligible [13] and best fit parameters are not affected by this kind of systematic errors.

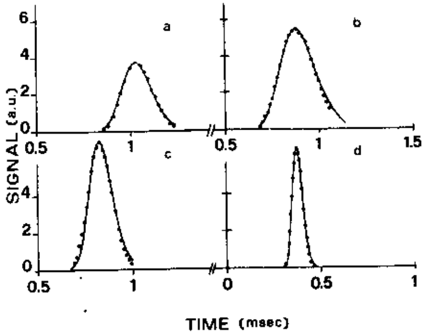

Fig. 4a–d. Experimental time-of-flight spectra of SF_6 (points) taken by a mechanical chopper (a) or by a pulsed CO_2 laser, tuned on the P(20) line (b, c, and d). The calculated spectra are shown by full lines. Experimental conditions and best fit parameters are the following:
a) pure SF_6 at 12 atm., $u = 390$ m/s, $\alpha = 45$ m/s;
b) pure SF_6 at 2 atm., $u = 358$ m/s, $\alpha = 60$ m/s;
c) pure SF_6 at 12 atm., $u = 390$ m/s, $\alpha = 45$ m/s;
d) 5% SF_6 in He at 1.5 atm., $u = 878$ m/s, $\alpha = 91$ m/s.
Calculated curves have been normalized to fit the maximum of experimental data

A comment is necessary about the efficiency of bolometers when used for time-of-flight measurements. Assuming that the stiking coefficient of molecules on the bolometer surface is one, we can distinguish three contributions to the energy E, detected by the bolometer, for each impinging molecule [5b]

$$E = E_a + E_i + mv^2/2, \tag{2}$$

where E_a is the adsorption energy, E_i is the internal ro-vibrational energy and $mv^2/2$ is the kinetic term. This last contribution is, in most cases, the bigger one and, of course, it depends on the velocity. For this reason (1) should be corrected to take into account the variation of detection efficiency with velocity. A rough estimation can be obtained assuming that E_i is due essentially to the vibrational energy. In general this is slightly modified during the beam expansion. The calculation of E_a requires a detailed knowledge of the surface composition. In the case of highly condensable species E_a can be derived from the heat of vaporization of the solid at 3.7 K. In addition, a detailed evaluation is very difficult to carry out because the assumption of unitary stiking coefficient may not be true in some cases. The use of pulsed laser modulation eliminates this problem of velocity dependence of sensitivity. In fact, in this case a continuous flux of molecules impings on the bolometer and the signal depends only on the internal energy E_i with time. As soon before the change of internal energy induced by the laser irradiation has no effect on the other terms of (2). Kinetic and adsorption energies contribute to a dc level which is not detected.

Concluding Remarks

We have demonstrated the feasibility of time resolved laser-bolometric spectroscopy for measuring kinetic energy distributions of molecules in a selected internal state. This method may find wide application for beam diagnostics when the fast superconducting bolometer is coupled to a suitable pulsed infrared laser. In our opinion an optical parametric oscillator [11] (OPO) pumped by a Nd:YAG laser is a good choice for this application. It gives a typical line width up to 0.1 cm^{-1} in the spectral range from about 1 to 20 µm. Although the frequency resolution is quite poor when compared to other tunable infrared sources, its frequency resolution is sufficient to resolve individual ro-vibrational transitions of simple molecules. In the case of complex molecules only a band contour can be resolved. On the other hand, if complex molecules are studied, an increase in resolution leads to a drastic reduction of the signal, due to statistical distribution of the molecules in the different states. Nevertheless the measurement of unresolved band contours is sufficient for evaluating the internal energy distribution. The power level of OPO lasers varies depending on the frequency, but is generally higher than 1 kW, and therefore, well over the limit to saturate the molecular beam absorption. Consequently, laser-bolometric measurements do not require power level correction and data analysis is drastically simplified.

It is now worth to compare time resolved laser-bolometric techniques with other diagnostic methods based on laser induced fluorescence (L.I.F.). In the latter experiments the fluorescence spectrum is measured after a laser induced electronic excitation of the molecule [14]. The L.I.F. technique is very promising although its general application so far has been limited by the need of suitable uv laser sources. Informations about kinetic energy distribution of molecules can be obtained by time resolved L.I.F. [17]. The T.O.F. between the region where the beam is optically pumped and that where it is state analyzed gives the kinetic energy. The kinetic energy distribution can be also obtained from detuning measurements when the crossing angle between the laser and the molecular beam is different from 90° [15]. The same effect has been applied to conventional laser-bolometric measurement to achieve velocity resolution [10]. The main advantage of Doppler detuning is the possibility of performing point analysis of velocity distribution and therefore to avoid the losses due to long flight paths. Moreover, all the molecules with a selected velocity contribute to the signal. On the contrary, a very poor duty cycle is obtained when the time resolved techniques are used. Where it is practicable the use of a pulsed molecular beam source [16], would avoid such a problem. The disadvantages of Doppler detuning methods are the critical dependence of velocity calibration on geometrical factors and the need of tunable lasers with narrow and stable lines. As observed before an increase in the resolution of the laser leads to a decrease in the signal when the molecules are distributed over a high density level spectrum.

When the goal of the experiment is diagnostics and not spectroscopy, the increase in resolution is a disadvantage. From the above considerations we may conclude that time resolved laser-bolometric techniques seems to be a convenient choice for molecular beam diagnostics, expecially when complex molecules are under investigation.

Acknowledgements. It is a pleasure to thank Dr. Gaetano Gallinaro for having provided us detailed informations about the fast bolometer construction, Dr. Giacinto Scoles for having stimulated our interest in laser-bolometric spectroscopic experiments and Dr. Salvatore Iannotta for his contribution to the development of this experiment and for very useful discussions. Thanks are also due to Dr. Bob Watkins, who kindly revised the manuscript. It is finally our pleasure to acknowledge the friendly and expert cooperation of the mechanical and cryogenic staff of the Physics Department at Trento.

References

1. See, for example *Atom-Molecule Collision Theory. A Guide for Experimentalist*; ed. by R.B.Bernstein (Plenum Press, New York 1979)
2. See, for example M.A.D.Fluendy and K.P.Lawley: *Chemical Applications of Molecular Beam Scattering* (Chapman and Hall, London 1973)
3. W.S.Young: Rev. Sci. Instrum. **44**, 715 (1973)
4. F.E.Bartoszek, D.M.Manos, J.C.Polanyi: J. Chem. Phys. **67**, 3395 (1977)
5. See, for example a) M.Cavallini, G.Gallinaro, G.Scoles: Z. Naturforsch. **22a**, 413 (1967);
   b) A.Schutte, D.Bassi, F.Tommasini, A.Turelli, G.Scoles, L.J.F.Hermans: J. Chem. Phys. **64**, 4135 (1976);
   c) M.Anderle, D.Bassi, S.Iannotta, S.Marchetti, G.Scoles: Phys. Rev. A **23**, 34 (1981)
6. G.Gallinaro, R.Varone: Cryogenics **15**, 292 (1975)
7. G.Gallinaro, G.Roba, R.Tatarek: J. Phys. E **11**, 628 (1978)
8. T.E.Gough, R.E.Miller, G.Scoles: a) Appl. Phys. Lett. **30**, 338 (1977); b) J. Mol. Spectrosc. **72**, 124 (1978); c) J. Chem. Phys. **69**, 1588 (1978)
9. D.Bassi, A.Boschetti, S.Marchetti, G.Scoles, M.Zen: J. Chem. Phys. 74, 2221 (1981)
10. R.E.Miller: Thesis, University of Waterloo, Waterloo, Ont. Canada, 1980 (unpublished)
11. S.J.Brosnan, R.L.Byer: IEEE J. QE-**15**, 415 (1979)
12. D.R.Coulter, F.R.Grabiner, L.M.Casson, G.W.Flynn, R.B. Bernstein: J. Chem. Phys. **73**, 281 (1980)
13. D.Bassi, A.Boschetti, G.Scoles, M.Scotoni, M.Zen: Proc. VIII International Symposium on Molecular Beams Cannes (1981)
14. a) M.P.Sinha, A.Schultz, R.N.Zare: J. Chem. Phys. **58**, 549 (1973);
    b) K.Bergmann, W.Demtröder, P.Heving: Appl. Phys. **8**, 65 (1975);
    c) R.E.Smalley, D.H.Levy, L.Wharton: J. Chem. Phys. **64**, 3266 (1976);
    d) P.J.Dagdigian: J. Chem. Phys. **64**, 2609 (1976);
    e) C.Y.R.Wu, J.B.Gooks, S.C.Yang, K.R.Way, W.C.Stwalley: Rev. Sci. Instrum. **49**, 380 (1979)
15. J.L.Kinsey: J. Chem. Phys. **66**, 2560 (1977)
16. D.Bassi, S.Ianotta, S.Niccolini: Rev. Instrum. **52**, 8 (1981)
17. a) T.D.Gaily, S.D.Rosnen, R.A.Holt: Rev. Sci. Instrum. **47**, 143 (1976);
    b) K.Bergmann, U.Hefter, P.Hering: J. Chem. Phys. **65**, 488 (1976);
    c) K.Bergmann, U.Hefter, P.Hering: Chem. Phys. **32**, 329 (1978)

OPTICS COMMUNICATIONS

SUPERSONIC BEAM SPECTROSCOPY OF LOW-J TRANSITIONS OF THE ν_3 BAND OF SF_6: RABI OSCILLATIONS AND ADIABATIC RAPID PASSAGE WITH A CW LASER ☆

S. AVRILLIER, J.-M. RAIMOND and Ch.J. BORDÉ,
Laboratoire de Physique des Lasers (Associé au C.N.R.S. no 282), Université Paris-Nord,
93430 - Villetaneuse, France

D. BASSI and G. SCOLES *
Istituto per la Ricerca Scientifica e Tecnologica and Unitá CNR - GNSM, Dipartimento di Fisica,
Università di Trento, 38050 - Povo (TN), Italia

Received 1 July 1981

The P(3) and P(4) manifolds of the ν_3 band of SF_6 have been observed in a supersonic beam with a bolometric detection. The influence of the laser beam divergence on the excitation efficiency has been studied. Rabi oscillations are observed when the wavefront is flat in the interaction region whereas only adiabatic rapid passage occurs when the molecules see a curved wavefront.

We have applied the cryogenic bolometer method of detection of vibrationally excited molecules in supersonic beams [1] to the spectroscopy of SF_6 in the 10 μm spectral region. The P(3) and P(4) manifolds of the ν_3 band which are in good coincidence respectively with the R(10) line of the N_2O laser and the P(16) line of the CO_2 laser [2] appeared to us as the most suitable choice for such an experiment, given the low rotational temperature in a supersonic beam. Fig. 1 is the schematic diagram of the experiment and fig. 2 shows the bolometer signal corresponding to the A_2 and F_2 components of the P(3) manifold when a helium beam seeded with 7% of SF_6 is illuminated by the N_2O laser. The comparison with a room temperature saturation spectrum confirms the assignment of these low *J* transitions. Recently we have obtained similar results with a waveguide CO_2 laser for the A_1, F_1 and E components of the P(4) manifold respectively at 228.154, 245.080 and 257.116 MHz from $Q(38)E^0$ [2].

We have used the P(3) A_2 line to perform a detailed quantitative study of the influence of the interaction geometry on the linewidth and excitation efficiency. The laser beam divergence has been varied by tuning the position of the second lens of a telescope. Fig. 3 shows the bolometer signal as a function of this position for three laser intensities. For these experiments the laser frequency was locked to the center of the line using saturation spectroscopy in an auxiliary cell. Because of the Doppler detuning only a fraction of the molecular beam velocity distribution along the optical axis interacts with the light. The signal is proportional to the width of the hole burnt in this distribution. This width is dominated by transit effects (including amplitude and phase modulation in a curved gaussian beam). The signal is thus minimum for minimum transit broadening, that is when the telescope focusing is perfectly adjusted and it reaches a maximum when the molecular beam and laser beam divergences are matched.

To account for the experimental data of fig. 3 we

☆ Work supported in part by D.R.E.T.

* Permanent address: Physics and Chemistry Department, University of Waterloo, Waterloo, Ontario, Canada, N2L 3G1.

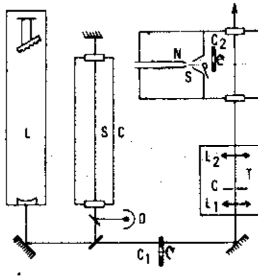

Fig. 1. Schematic diagram of the experiment. The molecular beam machine consists of two separate chambers each with its own diffusion pump. Gases are expanded through the 90 μm diameter nozzle (N) followed by a 0.5 mm diameter skimmer (S) into the second chamber equipped with a liquid-N_2 trap (Combined pumping speed of 1200 l/s). The operating pressures in the two chambers are respectively a few 10^{-4} Torr and a few 10^{-6} Torr. A beam flag and a chopper (C_2) are used for full beam intensity measurements. The bolometer (B) located 50 cm from the nozzle is mounted in contact with the cold surface of a liquid He Dewar. Its responsivity is 7×10^{-3} VW^{-1} and the RMS noise at 4.2K is 100 nV $Hz^{-1/2}$. The cw N_2O laser (L) is a conventional low pressure laser. Saturated absorption in an auxilliary cell (SC) is used to control the frequency tuning or to lock this frequency to the center of any observed resonance. The laser beam chopped by C_1 at a frequency around 30 Hz is expanded with a telescope (T) and spatially filtered with a pinhole (C) before its interaction with the molecular beam. The focal length of the two lenses of the telescope (L_1 and L_2) are respectively F_1 = 10 cm and F_2 = 33 cm.

found it necessary to use a non-perturbative calculation of the interaction between the molecules and the gaussian laser beam based on the equations of reference [4]. This theory shows that, in the strong field regime, the transition probability averaged over the

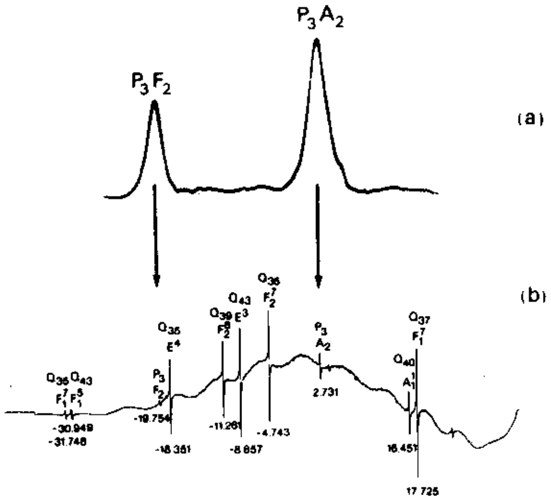

Fig. 2. SF_6 spectra obtained with the R(10) N_2O line; (a) supersonic beam (7% SF_6 in helium, source stagnation pressure 1.8 bar), (b) saturation spectrum in a room temperature cell. Frequencies are in MHz from the N_2O line center [2]. The absolute frequency of Q(37) F_1^7 is 28414593720 kHz [3].

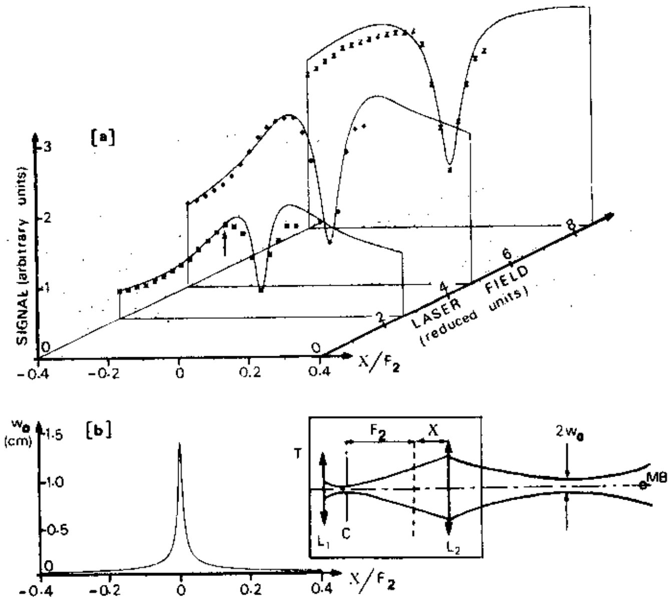

Fig. 3. (a) Excitation efficiency as a function of the laser focusing (position of the second lens of the telescope in units of focal length F_2 = 33 cm with respect to focal position) for laser powers respectively equal to 1.8, 6. and 19.4 mW. The only adjustable parameter of the set of calculated curves (solid lines) has been the signal amplitude for the point indicated by the arrow.
(b) Gaussian laser beam 1/e radius w_0 as a function of the laser focusing.

velocity distribution undergoes Rabi oscillations only when the laser field has minimum curvature in the interaction region for reasons to be discussed below.

To demonstrate these oscillations with a good enough signal-to-noise ratio we had to increase the number of interacting molecules without introducing curvature that is when the telescope is afocal and for this we modified the telescope to reduce the beam waist radius to 3 mm when located on the molecular beam (in fig. 1, the focal length F_2 was changed to 6.7 cm).

In fig. 4a we give experimental evidence that such oscillations do occur when the c.w. laser field strength is varied. The oscillations disappear for highest fields owing to the transverse field distribution and to the existence of three different Clebsch-Gordan coefficients in the dipole moment and are well represented by the theory.

When the laser beam waist is slightly offset from the molecular beam, i.e. when the molecules see curved wave-fronts, the Rabi oscillations disappear as illustrated in fig. 4b. The reason is that, as they travel across a curved gaussian beam, molecules see a linear sweep of the instantaneous frequency which induces a rapid adiabatic passage [5] if the field is strong enough. This rapid adiabatic passage inverts the medium without possibility for a complete Rabi precession as illustrated on the pseudo-spin [6] trajectories given in fig. 5. This doubles the available signal from the case where populations would be simply equalized. A detailed description of the coherent interaction between a gaussian laser beam and a supersonic molecular beam will be presented in a further paper.

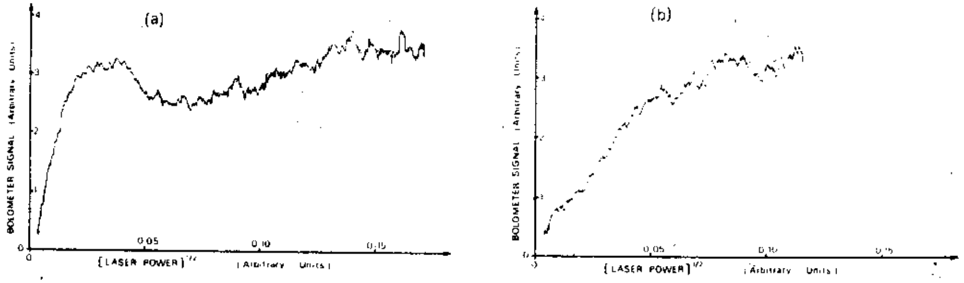

Fig. 4. (a) Rabi oscillation of the holometer signal as a function of the laser field. The laser is locked to the P(3) A_2 line center and the laser beam waist ($w_0 \approx 3$ mm) is accurately set on the molecular beam. The horizontal scale is roughly in $(\mathrm{Watt})^{1/2}$.
(b) Same as (a) but the laser beam waist is slightly offset from the molecular beam (the second lens of the telescope was moved by 0.5 mm with respect to (a).

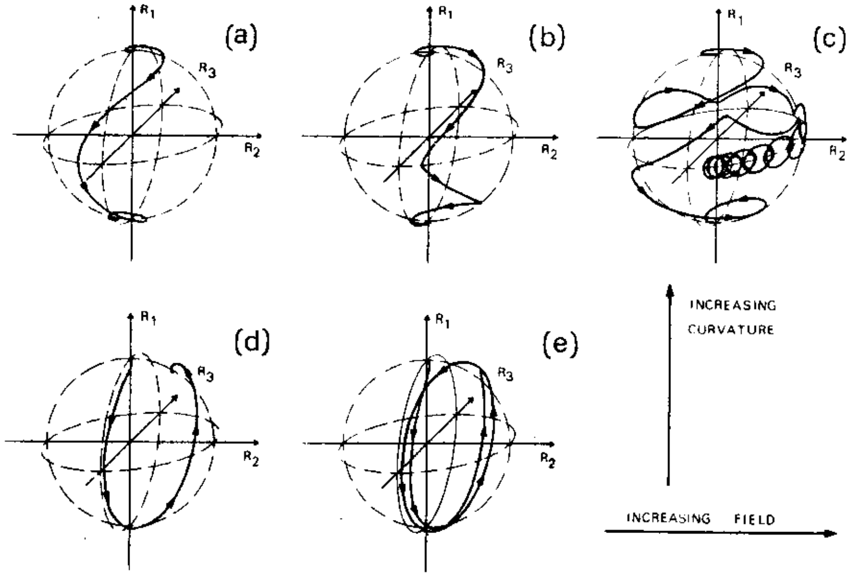

Fig. 5. Pseudo-spin trajectories in a gaussian laser beam calculated from the equations of ref. [4] with a predictor-corrector method. $R_1 = \rho_{bb} - \rho_{aa}$, $R_2 = 2\mathrm{Re}\,\rho_{ba}$ and $R_3 = 2\mathrm{Im}\,\rho_{ba}$. For (a), (b) and (c) the radius of curvature in units of half confocal parameter $2R/b = 3.55$ and $w^2/w_0^2 = 11.48$. For (d) and (e), $2R/b = 4.25$ and $w^2/w_0^2 = 1.06$. The Rabi frequency in units of reduced transit time $(\mu E_0/2\hbar)$ (w_0/u) is respectively 1.8 for (a) and (d), 3.4 for (b) and (e) and 39 for (c). For (d) and (e) the curvature is small enough for Rabi precession to occur. For (a), (b) and (c) adiabatic rapid passage inverting the populations takes place; the only effect of a field increase is to complexify the trajectory between the two poles.

A quantitative understanding of the excitation efficiency should be useful to most physical chemistry studies combining molecular beams and lasers. Furthermore the possibility to produce vibrationally excited SF_6 in states of well-defined symmetry should be specifically of interest to reactive scattering studies with this molecule.

References

[1] T.E. Cough, R.E. Miller and G. Scoles, Appl. Phys. Lett. 30 (1977) 338.
[2] A. Van Lerberghe, S. Avrillier and Ch.J. Bordé, IEEE J. Quantum Electron. 14 (1978) 481;
C. Salomon, A. Van Lerberghe and Ch.J. Bordé, to be published.
[3] A. Clairon, A. Van Lerberghe, C. Salomon, M. Ouhayoun and Ch.J. Bordé, Optics Comm. 35 (1980) 368.
[4] Ch.J. Bordé, J.L. Hall, C.V. Kunasz and D.G. Hummer, Phys. Rev. 14 (1976) 236.
[5] A. Abragam, Principles of nuclear magnetism (Oxford University Press, New York, (1961).
[6] R.P. Feynman, F.L. Vernon and R.W. Hellwarth, J. Appl. Phys. 28 (1957) 49.

OBSERVATION OF OPTICAL RAMSEY FRINGES IN THE 10 µm SPECTRAL REGION USING A SUPERSONIC BEAM OF SF_6 (*)

Ch. J. Bordé, S. Avrillier, A. Van Lerberghe, Ch. Salomon, D. Bassi (**)
and G. Scoles (**) (+)

Laboratoire de Physique des Lasers (Associé au C.N.R.S., L.A. 282),
Université Paris-Nord, Avenue J.B. Clément, 93430 Villetaneuse, France

(**)Istituto per la Ricerca Scientifica e Tecnologica and Unità CNR-GNSM,
Dipartimento di Fisica, Università di Trento, 3805 Povo (TN), Italia.

Abstract : We report a first observation of optical Ramsey fringes in the 10 µm spectral region using a supersonic seeded beam of 7% SF_6 in He, illuminated by a CO_2 laser in spatially-separated field zones. We have used either three standing waves or four travelling waves and obtained highly contrasted fringes with a 23 kHz half-width corresponding to a 5 mm distance between zones.

Laser excitation of the vibrational energy of molecules in a beam can be conveniently detected with a cryogenic bolometer [1] and a demonstration of this technique in the case of the ν_3 mode of SF_6 excited by CO_2 or N_2O lasers has been recently given [2] . With this equipment the spatial analog of coherent transient effects such as the Rabi oscillations of the transition probability and the adiabatic rapid passage were shown to occur respectively with plane and curved wavefronts. In an attempt to investigate the potential use of this method for very high resolution spectroscopy and optical frequency standards we have made a preliminary experiment to detect the Ramsey fringes associated with saturation spectroscopy in an interaction geometry comprising three or four field zones [3-14].

For this experiment we used the P(4) F_1 and E components of the ν_3 band of SF_6 which can be reached with a waveguide CO_2 laser oscillating on the P(16) CO_2 line at 10.55 µm. To control the frequency of this laser we locked it, with a tunable frequency offset, to a conventional reference laser locked to the Q(45) F_2^7 SF_6 line. The beam from the waveguide laser was spatially filtered and magnified to have a waist of $w_o = 6$ mm. In the case of illumination by this single beam the resulting width (FWHM) of the observed line was a combination of transit broadening and residual first-order Doppler effect along the optical axis and amounted to 300 kHz.We used the Rabi oscillation to set the laser beam waist precisely on the molecular beam [2]. Four oscillations of the signal could be observed with a 40% contrast with successive minima obtained for a total power of ∿1,4,9 and 16 mW.

To obtain fringes,part of the laser beam was intercepted before the interaction region by a screen which transmitted the light only through 1 mm wide slits. Two different geometries were used in these experiments. In the first one, three equidistant standing waves were generated by three equidistant slits of 5 mm separation together with a corner cube placed on the other side of the molecular beam to retroreflect the light back through the slits. In the second geometry, only two of the previous slits were illuminated. An offset between the center of the slits and the center of the corner cube generated two counter-propagating sets of travelling waves with a 5 mm distance between adjacent co-propagating waves of each set. The spacing between the two sets can be arbitrary and was actually 10 mm in this experiment. Highly contrasted fringes have been obtained in both cases and as an example the figure displays the signal corresponding to the four travelling waves case. Use of purely travelling waves to obtain optical Ramsey fringes has been suggested by the analysis of references [4-5,10] and we have here a first demonstration of this possibility together with the Ca beam experiment of Helmcke et al.[14] . The broad pedestal has a width ∿1.4 MHz corresponding to the transit broadening width across a single zone. The fringes themselves have a 23 kHz width (HWHM) consistent with a ∿930 m/sec peak velocity of the SF_6 molecules [15].

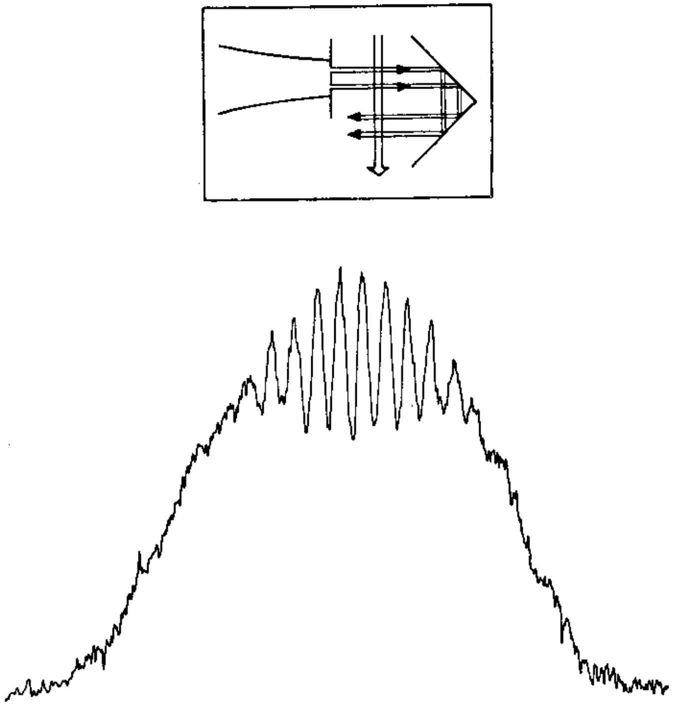

Figure 1. :

Ramsey pattern obtained for P(4)F_1 SF_6 line with four travelling waves (interaction geometry illustrated by the inset). The horizontal scale is linear in frequency and one fringe period corresponds to 92.5 kHz. The total laser power before the slits was 18 mW. The signal was recorded in a single one minute sweep with a 0.1 second time constant and a 30 Hz modulation frequency of the laser amplitude.

(*)Work supported in part by D.R.E.T.

(+)Permanent address : Physics and Chemistry Department, University of Waterloo, Waterloo, Ontario, Canada, N2L 3G1.

We have the choice between various mathematical tools for the theoretical description of these experiments. The approaches which have been used in the past are either perturbative calculations using density matrix diagrams or numerical treatments of the density matrix equations in the strong field case [4,5]. Another powerful tool is the 2x2 matrix formalism presented at this conference [16]. Since it applies very well to the present experiment it is worth giving here a brief outline of this theory.

The evolution operator for the two-component spinor $\begin{pmatrix} b \\ a \end{pmatrix}$ describing a two-level system is written :

$$\mathscr{U}(t,t_o) = \mathscr{T}\exp\left\{\int_{t_o}^{t}\left(\frac{H(t')}{i\hbar} - \frac{\Gamma}{2}\right) dt'\right\}$$

where $H = \begin{pmatrix} E_b & 0 \\ 0 & E_a \end{pmatrix} + V(t)$ and $\Gamma = \begin{pmatrix} \gamma_b & 0 \\ 0 & \gamma_a \end{pmatrix}$ are easily expanded on the basis of the Pauli matrices $I, \vec{\sigma}$.

The time-ordering operator $\mathscr{T}$ can be ignored either in the case of travelling waves with constant fields in each zone or in the case of standing waves with arbitrary transverse dependence of the fields.

In the first case the interaction hamiltonian V(t) is time-independent in a rotating frame (if we make the rotating wave approximation) :

$$-\frac{\mu E}{2}\begin{pmatrix} 0 & \exp(\pm ikz+i\varphi) \\ \exp(\mp ikz-i\varphi) & 0 \end{pmatrix}$$

The evolution operator reduces to a simple 2x2 matrix :

$$\begin{pmatrix} A & Be^{\pm ikz} \\ Ce^{\mp ikz} & D \end{pmatrix} = \exp\left\{\left(-i\,\frac{E_a+E_b}{2\hbar} - \frac{\gamma_{ba}}{2}\right)(t-t_o)I\right\}\left[I\cos\frac{\Omega(t-t_o)}{2} + i\,\frac{\vec{\Omega}.\vec{\sigma}}{\Omega}\sin\frac{\Omega(t-t_o)}{2}\right]$$

where $\vec{\Omega} = \left(-\frac{\mu E}{\hbar}\cos(kz+\varphi),\ \mp\frac{\mu E}{\hbar}\sin(kz+\varphi),\ \Omega_o \mp kv_z + i(\gamma_b-\gamma_a)/2\right)$ is the effective field vector and with

$$\gamma_{ba} = (\gamma_b + \gamma_a)/2 \quad , \quad \Omega_o = \omega - \omega_o \quad , \quad \Omega^2 = \vec{\Omega}^2$$

With four travelling waves and molecules initially in state a, we obtain the final two-component spinor by simple multiplication of matrices :

$$\begin{pmatrix} A_4 & B_4e^{-ikz} \\ C_4e^{ikz} & D_4 \end{pmatrix}\begin{pmatrix} e^{i(\Omega_o+kv_z)T/2} & 0 \\ 0 & e^{-i(\Omega_o+kv_z)T/2} \end{pmatrix}\begin{pmatrix} A_3 & B_3e^{-ikz} \\ C_3e^{ikz} & D_3 \end{pmatrix}\begin{pmatrix} e^{ikv_z(t-T)} & 0 \\ 0 & e^{-ikv_z(t-T)} \end{pmatrix}$$

$$\begin{pmatrix} A_2 & B_2e^{ikz} \\ C_2e^{-ikz} & D_2 \end{pmatrix}\begin{pmatrix} e^{i(\Omega_o-kv_z)T/2} & 0 \\ 0 & e^{-i(\Omega_o-kv_z)T/2} \end{pmatrix}\begin{pmatrix} A_1 & B_1e^{ik_z} \\ C_1e^{-ik_z} & D_1 \end{pmatrix}\begin{pmatrix} 0 \\ 1 \end{pmatrix}$$

where T is the time of flight between the first two and last two field zones. For the sake of simplicity we have taken $\gamma_a = \gamma_b$ and we have ignored the time of flight between the two central zones but we have written explicitly the change of rotating frame between these two counter-propagating fields.

The part of the final upper level population representing the fringe pattern is simply :

$$bb^* = \left(A_4B_4^*A_3C_3^*A_2B_2^*B_1D_1^*e^{2i\Omega_oT} + A_4B_4^*B_3D_3^*C_2D_2^*B_1D_1^*e^{2i\Omega_oT} + c.c.\right)\exp(-2\gamma_{ba}T)$$

The Doppler phase cancels out because it reverses in the second dark zone. (It is easy to follow the corresponding trajectory of the pseudo-spin and this will be illustrated in another paper). The factors multiplying the oscillating terms $\exp\pm 2i\Omega_o T$ have to be numerically integrated over the v_z distribution to obtain the exact shape of the fringes envelope. Let us finally point out that when the field phases cancel out (which is the case in our experiment) the central fringe corresponds to a negative contribution.

In the case of standing-waves we cannot completely remove the time dependence of the interaction hamiltonian which is written (in the rotating frame at ω and in the molecular frame) :

$$V = -\mu E\cos(kz + kv_zt + \varphi)\ U(\vec{r} + \vec{v}t)\ \sigma_x$$

where $U(\vec{r})$ is the transverse dependence of the field in each zone.
The only possibility to reduce the total hamiltonian to an operator commuting with itself at different times is to neglect the σ_z term during the interaction with the field. The evolution operator is then simply :

$$I\cos\Phi + i\sigma_x\sin\Phi$$

$$\text{with} \qquad \Phi = \frac{\mu E}{\hbar}\int_{-\infty}^{+\infty}U(t)\cos(kv_zt + kz + \varphi)dt$$

The time evolution of the two-component spinor is again described by the product of matrices corresponding to the five zones and the final result for the oscillating part of bb* has the following form already derived by Dubetsky [6] with a different approach :

$$bb^* = \frac{1}{4}\exp(-2\gamma_{ba}T)\cos 2\Omega_oT\sin 2\Phi_3\cos 2\Phi_2\sin 2\Phi_1$$

This formula displays the oscillation character but, unfortunately, does not have the simplicity of the travelling wave case since further integration on both z and v_z are required to obtain the signal.

A detailed comparison of the observed line profiles with calculated ones is presently under way. The predicted apparent splitting of the fringe pattern in a strong field has been observed in the three-slit experiment and is also being investigated.

We expect now to be able to increase significantly the resolving power with Gaussian zones separated by much larger distances using the corner cube techniques described in [17]. Let us finally point out that a major advantage of supersonic beams for an optical frequency standard is the good monochromaticity in velocity space yielding a well-defined second-order Doppler shift.

REFERENCES

[1] GOUGH T.E., MILLER R.E. and SCOLES G., Appl. Phys. Lett. 30, 338 (1977).

[2] AVRILLIER S., RAIMOND J.-M., BORDÉ Ch.J., BASSI D., SCOLES G., Opt. Comm. (in press) (1981) and to be published.

[3] BAKLANOV Ye.V., DUBETSKY B. Ya. and CHEBOTAYEV V.P., Appl. Phys. 9, 171(1976).

[4] BORDÉ Ch.J., C.R. Acad. Sc. Paris 284B, 101 (1977).

[5] BORDÉ Ch.J., in Laser Spectroscopy III, p.121, edited by J.L. HALL and J.L. CARLSTEN, Springer Verlag (1977).

[6] DUBETSKY B.Ya, Sov. J. Quantum Electron. 6, 682 (1976).

[7] DUBETSKY B.Ya and SEMIBALAMUT V.M., Sov. J. Quantum Electron. 8, 103 (1978).

[8] HATA N. and SHIMODA K., Appl. Phys. 22, 1 (1980).

[9] BERGQUIST J.C., Ph.D. Thesis, University of Colorado (1978).

[10] BERGQUIST J.C., LEE S.A. and HALL J.L., Phys. Rev. Lett. 38, 159 (1977).

[11] BARGER R.L., BERGQUIST J.C., ENGLISH T.C. and GLAZE D.J., Appl. Phys. Lett. 34, 850 (1979).

[12] BARGER R.L. Opt. Lett. 6, 145 (1981).

[13] BABA M. and SHIMODA K., Appl. Phys. 24, 11 (1981).

[14] HELMCKE J., GLASER M., ZEVGOLIS D. and YEN B.Ü., Third Symposium on Frequency Standards and Metrology, Aussois, France (Oct. 1981).

[15] BASSI D., Private Communication.

[16] BORDÉ Ch.J., Third Symposium on Frequency Standards and Metrology, Aussois, France (Oct. 1981).

[17] SALOMON Ch., BREANT Ch., BORDÉ Ch.J. and BARGER R.L., this issue.

INFRARED MULTIPLE PHOTON EXCITATION OF SULFUR HEXAFLUORIDE IN A MOLECULAR BEAM

D. BASSI, A. BOSCHETTI, G. SCOLES *, M. SCOTONI
Dipartimento di Fisica, Università di Trento, 38050 Povo (TN), Italy

and

M. ZEN
Istituto per la Ricerca Scientifica e Tecnologica, 38050 Povo (TN), Italy

Received 30 April 1982

The infrared multiple photon excitation of SF_6 in a supersonic molecular beam has been investigated by means of the laser–bolometric technique. In this experiment molecules are irradiated below dissociation threshold in a true collisionless regime. The absorbed energy is detected by means of a fast superconducting bolometer. The molecular beam is obtained by expanding pure SF_6 and SF_6 seeded in helium or argon at different pressures. The multiple photon excitation spectra are very sensitive to the molecular beam conditions. Spectra become narrower as the pressure is increased. This effect has been attributed mainly to the rotational cooling which occurs during beam formation.

1. Introduction

Interest in laser selective chemistry and isotope separation has, in recent years, spurred extensive experimental and theoretical investigations of infrared multiple photon excitation (MPE) and dissociation of polyatomic molecules (see, for example, ref. [1]). It is difficult to summarize in a few words the main results obtained in this fast growing research field. In general we can say that a complete quantitative description of MPE is not yet available, but some important points are now well established. The reason for that is to be found in the complexity of the energy level schemes of the molecules involved in the first few MPE processes. It is known that the first vibrational levels play the main role to determine the excitation selectivity. The experimental observation of narrow resonances in the MPE spectrum [2] together with a better theoretical description of the rovibrational ladder [3] can contribute to further clarify this point. The relationship between peak laser power, fluence and excitation has been studied in detail elsewhere [4]. It has recently been demonstrated that the generally accepted energy fluence scaling law fails when the peak power is larger than ≈200 MW cm^{-2} [4b]. New experimental methods have recently been introduced to improve the accuracy of MPE measurements [5,6]. One of the aims of these new techniques is to clearly separate the collisionless excitation from collision effects. Collisions are the source of specific effects in cell experiments especially when long laser pulses are used [7]. Other errors can originate from photon absorption from molecular fragments and by self-focusing of radiation along the cell path [8].

It is well known that these effects are not present in molecular beam experiments and, indeed, this technique, together with mass spectrometry, has been successfully used to study the multiple photon dissociation of polyatomic molecules [9]. To extend molecular beam studies below the dissociation threshold laser induced fluorescence has been proposed and tested [10]. This technique can give detailed information about the first steps of the excitation. Unfortunately,

---

[*] Permanent address: Department of Chemistry, University of Waterloo, Waterloo, Ontario, Canada N2L 3G1.

its wide application is limited by the need for suitable UV tunable lasers. The measurement of energy deposition is, in the infrared region of the spectrum, the logical alternative to the fluorescence excitation method.

With this in mind we decided to investigate the extension of the laser–bolometric technique [11] to pulsed laser excitation and apply it to the measurement of SF_6 MPE spectra. Up to now this technique has found several applications in infrared spectroscopy [12–15] and, in particular, it has been used to study the low J transitions of the ν_3 band of SF_6 [14]. The basic idea in laser–bolometric experiments, is to measure the energy absorbed by a molecular beam by means of a cryogenic bolometer. The result of the measurements is essentially the average number of photons absorbed by one molecule. Thus the results are directly comparable to the data obtained in cell experiments. There is a strong analogy between laser bolometric and opto-acoustic techniques [16]. Both of them are based on the measurement of the energy absorbed by the sample instead of the laser beam attenuation. However, in the beam the cooling of the internal degrees of freedom associated with the supersonic expansion can be utilized to vary the initial energy distribution of the molecules and to study its effect on MPE efficiency.

2. Experimental

The experimental apparatus, shown schematically in fig. 1, is a modified version of the molecular beam infrared spectrometer described in ref. [15]. In the present configuration the IR source is a Lumonics TEA 820 tunable CO_2 laser. It produces multimode 2 J pulses, operating at a maximum repetition rate of 20 pps. About 50% of the energy is released during the first 100 ns of the pulse, followed by the usual nitrogen tail. The laser beam is focused on the molecular beam by means of a cylindrical lens (focal length 30 cm). The irradiated region is 1.6 cm long. The energy density can be varied by changing the lens position without affecting the length of the irradiated region. A variable attenuator is inserted between the laser and the lens to equalize the intensity of different laser lines.

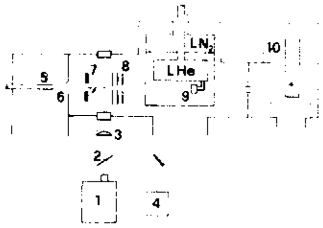

Fig. 1. Experimental apparatus: (1) TEA CO_2 laser; (2) variable attenuator; (3) cylindrical lens; (4) laser detector or spectrum analyzer; (5) supersonic beam source; (6) skimmer; (7) chopper; (8) optical baffle; (9) bolometer; (10) mass spectrometer.

The molecular beam is obtained by supersonic expansion of pure SF_6 and SF_6 seeded in helium or argon, through a room temperature nozzle of $(30 \pm 3) \times 10^{-4}$ cm diameter. The density of SF_6 molecules in the beam can be monitored by means of a quadrupole mass spectrometer.

The molecular beam detector is a fast superconducting bolometer [17]. The detection system is described in detail in ref. [18]. The detector has a rectangular shape (1×4 mm^2) and is located 33.5 cm downstream of the center of the irradiation region. We take advantage of the fast response time of the superconducting bolometer to separate the spurious signal due to electromagnetic interferences and diffused infrared radiation from the signal due to vibrationally excited molecules. The spurious signal is synchronous with the laser pulse while the molecular one has a delay corresponding to the time of flight of the excited molecules from the excitation region to the detector. In a typical measurement we resolve the time dependence of the bolometric signal $S_L(t)$ by means of electronic averaging the contribution of 100 successive pulses. The area under the signal is proportional to the energy absorbed by the molecular beam. We have measured the integral bolometric signal as a function of laser frequency and source pressure. The bolometer and the quadrupole mass spectrometer are both used to obtain the calibration of the average number of photons absorbed by one molecule. The first step consists in measuring the intensity of a mechanically chopped pure SF_6 beam by means of the bolometer. The signal S_B is given by

$$S_B = \alpha\phi R(E_T + E_A)\,, \tag{2.1}$$

where α is a geometric parameter, ϕ is the molecular beam flux and R is the bolometer responsivity. The energy $E_T + E_A$ is the sum of E_T, the total energy per beam molecule, and E_A, the adsorption energy of SF_6 on the bolometer surface. The value of $E_T + E_A$ has been chosen equal to 5.6×10^{-20} J in agreement with the evaluation of ref. [23]. After this measurement the mechanical chopper is stopped in its open position. The beam is irradiated by the pulsed laser and the signal $S_L(t)$ is measured. We can write

$$I = \int S_L(t)\,dt = \alpha\phi R\langle N\rangle E_\nu L/\langle v\rangle\,, \tag{2.2}$$

where L is the length of the illuminated region and $\langle v\rangle$ is the average velocity of SF_6 molecules. The geometric parameter α in eqs. (2.1) and (2.2) is the same because the dimension of the laser spot in the irradiation region is larger than the molecular beam diameter. The value $\langle v\rangle$ is obtained by analysis of the time dependence of $S_L(t)$ [18]. The product $\alpha\phi L/\langle v\rangle$ gives the number of molecules impinging on the bolometer after being exposed to the laser pulse. Of course we assume that there is no loss of molecules due to photodissociation effects. This condition is satisfied if the laser fluence is set below the multiple photon dissociation threshold and if dimers or higher clusters are absent from the beam. The latter condition will further be discussed in more detail. The energy E_ν which appears in eq. (2.2) is the energy of one 10.6 μm photon. The average number of photons absorbed by one molecule $\langle N\rangle$ is then obtained as

$$\langle N\rangle = \frac{E_T + E_A}{E_\nu}\,\frac{I}{S_B}\,\frac{\langle v\rangle}{L}\,. \tag{2.3}$$

This calibration cannot be applied directly to seeded beams because in this case we do not know in detail the concentration of heavy molecules in the beam and the energy distribution among SF_6 and the carrier gas [20]. To overcome this problem we have used a relative calibration. The seeded molecular beam is mechanically chopped and its intensity is measured by means of the mass spectrometer instead of the bolometer. The mass spectrometer is tuned on the SF_5^+ mass and gives a signal S_S proportional to the SF_6 density in the beam

$$S_S \propto \phi/\langle v\rangle\,. \tag{2.4}$$

The ratio I/S_S is proportional to $\langle N\rangle$.

We get

$$\langle N\rangle = KI/S_S\,. \tag{2.5}$$

The proportionality constant K is independent of the beam velocity $\langle v\rangle$ and is the same for all types of SF_6 mixtures. The actual value of K is determined by means of a pure SF_6 beam which has been independently calibrated by means of eq. (2.3), under the same laser conditions. When the source operates with seeded mixtures the maximum operating pressure is limited by condensation effects. Dimers and higher-order clusters may be produced during the expansion. After laser irradiation these species undergo vibrational predissociation [19]. As a consequence the bolometric signal is decreased by the negative contribution of the fragments leaving the beam. This effect has been previously used with cw lasers to measure the vibrational predissociation spectrum of N_2O and CO_2 dimers [13]. An example of such behaviour is shown in fig. 2.

At high pressures (fig. 2a) a negative signal is measured when the laser is tuned at the P(10) CO_2 line. This frequency is far from the range defined by the MPE spectrum [16], but is near a peak of the broad vibrational predissociation spectrum of SF_6 dimers and clusters [19]. When the pressure is reduced the negative signal disappears (fig. 2c). We can conclude that the signal of fig. 2a is an indication of the presence of polymeric species in the beam. If the laser is tuned at the P(18) CO_2 line, near the maximum of the MPE spectrum, a different behaviour is observed. The high

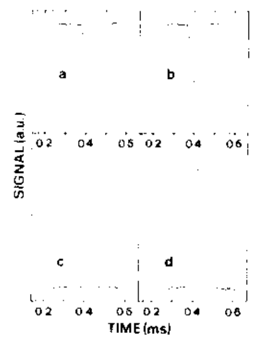

Fig. 2. Time-resolved bolometric signal for 10% SF_6 seeded in helium. (a) Source pressure 10 atm, P(10) CO_2 laser line. (b) Source pressure 10 atm, P(18) CO_2 laser line. (c) Source pressure 2.5 atm, P(10) CO_2 laser line. (d) Source pressure 2.5 atm, P(18) CO_2 laser line.

pressure signal (fig. 2b) becomes the sum of two opposite contributions. In the example shown the vibrational predissociation is dominant and the net signal is negative. When the source pressure is reduced (fig. 2d) and the concentration of polymeric species becomes negligible a positive MPE signal is observed.

To avoid any interference from the dissociation of dimers and higher clusters in MPE measurements we have limited our investigation to source pressures where the negative vibrational predissociation P(10) signal shown in fig. 2a is not detectable within our experimental error.

3. Results and discussion

In fig. 3 we show a few examples of MPE spectra taken with pure SF_6 and SF_6 seeded in helium or argon beams. During all these measurements the stagnation pressure of the molecular beam source was 2.5 atm and the laser fluence was set at 1 J cm^{-2}. This value was chosen well below the dissociation threshold [9] to avoid loss of signal due to fragments leaving the beam. We have observed a strong dependence of the MPE spectra from both the mixture used to produce the beam and from the source pressure. We have chosen the full width at half maximum (fwhm) as the parameter which summarizes, in a straightforward way, the modifications of the spectrum as a function of the source pressure. The corresponding results are shown in fig. 4. The arrow on the left part of this figure indicates the result obtained in a room temperature cell experiment under similar laser conditions [16]. The dependence of the average number of photons absorbed by one molecule as a function of the source pressure is shown in fig. 5 for a 10% SF_6 –He seeded beam, at two different CO_2 laser lines.

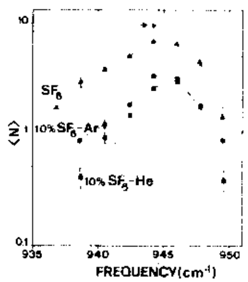

Fig. 3. Average number of photons absorbed (⟨N⟩) as a function of CO_2 laser frequency for pure SF_6 and SF_6 seeded in helium or argon beams. The molecular beam source operates at 2.5 atm. The laser fluence is 1 J cm^{-2}. The arrow indicates the value obtained in a room temperature cell experiment under similar laser conditions [4a].

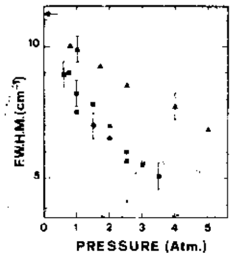

Fig. 4. Full width at half maximum (fwhm) of MPE spectra as a function of the molecular beam source pressure for different mixtures: ▲ pure SF_6; ● 10% SF_6 in argon; ■ 10% SF_6 in helium. The arrow on the left part of the figure corresponds to the value obtained in a room temperature cell experiment under similar laser conditions [16]. The laser fluence is 1 J cm^{-2}.

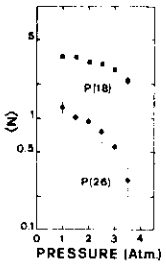

Fig. 5. Average number of photons absorbed for 10% SF_6 in helium at different source pressures. The CO_2 laser has been tuned on the P(18) and P(26) lines.

The dependence of our experimental data on the molecular beam source conditions can be explained by taking into account the relaxation of the internal degrees of freedom during the supersonic expansion [20]. Both rotational and vibrational temperatures will be reduced. The cooling efficiency depends on the energy gap involved in the process and from the number of collisions experienced by the molecule. This number is, in first approximation, proportional to the product of the source pressure with the nozzle diameter. In general vibrational relaxation occurs with difficulty. The relaxation of vibrationally excited SF_6 has been studied in detail in ref. [21]. The main results of this work are the following:

(a) About 1500 collisions are necessary to relax one ν_3 quantum in pure SF_6. The vibrational energy is quickly redistributed among all vibrational modes. The relaxation of excited vibrational levels is limited by the vibrational → translational relaxation of the lowest level (ν_6 at 347 cm^{-1});

(b) The relative deactivation efficiency for collisions between SF_6 and helium or argon compared to pure SF_6 is respectively 1.83 and 0.37.

We have calculated the average number of collisions for a pure SF_6 beam. The molecular beam expansion has been described by means of the isoentropic model [20]. The collision frequency varies along the jet center-line and can be expressed in terms of the local Mach number. We have used the model of ref. [24] to calculate the Mach number in the region $0 \leqslant x/D^* \leqslant 2$, where x is the distance from the nozzle throat and D^* is the effective nozzle diameter. For $x/D^* \geqslant 3$ the Ashkenas and Sherman approximation has been used [27]. A linear interpolation has been used to calculate the Mach number in the range $2 < x/D^* < 3$. The calculation has been performed using the following parameters: SF_6 hard-sphere diameter 5.4 Å [25], specific heat ratio $\gamma = 1.095$ [26], source temperature 293 K, source stagnation pressure 2.5 atm. Under these conditions we have found a total number of collisions near 800. To evaluate the vibrational temperature of SF_6 molecules, we have assumed that vibrational relaxation is proportional to the difference between vibrational T_V and translational T_{TR} temperatures [28]. The following rate equation can be written

$$dT_V/dx = -(\nu/uK)(T_V - T_{TR}) , \qquad (3.1)$$

where ν is the collision frequency, u is the bulk velocity and $K = 1500$ is the relaxation efficiency [21]. In this way we have estimated a final vibrational temperature of ≈270 K. From this result we have concluded that the vibrational distribution of SF_6 molecules is not significantly modified during the beam formation. A similar result has been obtained for seeded beams. In spite of the uncertainties in the vibrational temperature so determined the spectra narrowing shown in fig. 4 cannot be explained in terms of vibrational relaxation only. This is because we observe that beams seeded in helium or argon show spectra that have more or less the same fwhm as a function of pressure while helium is about five times more efficient with respect to argon for relaxing SF_6 vibrations. If the vibrational temperature of SF_6 is reduced from 300 to 270 K the fraction of molecules in the ground vibrational state increases from about 30 to 39%. A small fraction of molecules occupies the first excited ν_3 level. This fraction is always less than 1%. The other molecules are distributed over the remaining vibrational states and can contribute to the 10 μm absorbtion band by means of the "so-called" hot-bands. Most populated hot-bands are red-shifted with respect to the 0 → 1 ν_3 frequency of less than 2 cm^{-1} [29]. The presence of hot bands is expected to influence the multiple photon excitation spectrum because it increases the probability of the first vibrational excitation at frequencies lower than 948 cm^{-1}. However we know that excitation up to the quasicontinuum is allowed by the anharmonic splitting of the ν_3 states and that the rotational structure provides a fine tuning for multiple photon resonances [3]. Thus the modifications of the MPE spectrum as a function of the molecular beam conditions are, in our opinion, mainly due to rotational cooling. This result is not surprising because the multiplicity of rovibrational levels increases strongly with the rotational quantum number J. However, in our true collision-free regime rotational refilling cannot occur. Assuming that high J rotational levels contribute mainly to the red tail of the MPE spectrum, when rotational cooling depletes these high J states the spectrum becomes narrower. The reduction of ⟨N⟩ even on the maximum of the MPE spectrum (figs. 3 and 5) can be explained in terms of the reduced number of multiple photon pathways which are accessible to low J molecules. Of course we cannot exclude the presence of MPE resonances at some frequencies in between those accessible to our laser source.

It would be interesting to compare our experimental data with recently published model calculations based on thermally averaged rotational populations [3b] since this work shows significant effects when the rotational temperature is varied from 1 to 10 K. Unfortunately, the number of levels included in the calculation is limited and a comparison with experimental data is not yet possible.

4. Conclusions

The present work demonstrates the feasibility of investigating quantitatively, with the laser bolometric technique, the multiple photon excitation of molecules under a true collisionless regime. We have shown that SF_6 MPE spectra are very sensitive to the molecular beam source conditions. The observed spectra narrowing has been attributed mainly to the rotational cooling which occurs during beam formation. The linewidth reduction is accompanied by a decrease of MPE efficiency. This effect is probably due to the limited number of MPE resonances which are accessible to low J molecules. When rotational cooling is used to improve the selectivity of MPE for isotope separation applications, the relative reduction of MPE efficiency should be taken into account. To further clarify this point an improvement in molecular beam diagnostics is necessary. We plan to do experiments in this direction with a variable temperature molecular beam source coupled with direct measurements of rotational distributions by means of a diode laser [15]. Another important contribution could come from the extension of Raman experiments [22]. In our opinion molecular beam experiments could, in the future, lead to significant improvements in our knowledges of MPE phenomena. In particular the use of fully characterized molecular beams together with continuously tunable high power lasers will be very useful for the detailed study of the role played by the initial energy distribution in the laser excitation process.

Acknowledgement

This work has been made possible by the financial support from the Italian Ministery for the Public Education (MPI). It is a pleasure to thank Professor C.D. Cantrell and Professor J. Reuss for stimulating discussions. One of us (G.S.) would like to gratefully acknowledge several useful discussions with Professor T.E. Gough. It is finally our pleasure to acknowledge the friendly and expert cooperation of the mechanical and cryogenic staff of the Physics Department at Trento.

References

[1] (a) N. Bloembergen and E. Yablonovitch, Phys. Today 31 (1978) 23;
(b) V.S. Letokhov, Phys. Today 33 (1980) 34;
(c) R.W. Ambartzumian, C.D. Cantrell and A.A. Puretzky, Multiple photon laser chemistry (Springer, Berlin), to be published.
[2] (a) S.S. Alimpiev, N.V. Karlov, G.A. Mesyats, S.M. Nikiforov, V.M. Orlovskii, A.M. Prokhorov, B.G. Sartakov, E.M. Khokhlov and A.L. Shtarkor, JETP Letters 30 (1979) 259;
(b) I.N. Knyazev, N.P. Kuzmina, V.S. Letokhov, V.V. Lobko and A.A. Sarkisyan, Appl. Phys. 22 (1980) 429.
[3] (a) C.D. Cantrell, H.W. Galbraith and J. Ackerhalt, in: Multiphoton processes, eds. J.H. Eberly and P. Lambropoulos, (Wiley, New York, 1978);
(b) D.P. Hodgkinson, A.J. Taylor and A.G. Robiette, J. Phys. B14 (1981) 1803.
[4] (a) J.G. Black, P. Kolodner, M.J. Shultz, E. Yablonovitch and N. Bloembergen, Phys. Rev. A19 (1979) 704;
(b) H.S. Kwok, E. Yablonovitch and N. Bloembergen, Phys. Rev. A23 (1981) 3094.
[5] (a) H.S. Kwok and E. Yablonovitch, Phys. Rev. Letters 41 (1978) 745;
(b) R.C. Sharp, E. Yablonovitch and N. Bloembergen, J. Chem. Phys. 74 (1981) 5357.
[6] (a) V.N. Bagratashvili, Yu.G. Vainer, V.S. Doljikov, S.F. Koliakov, A.A. Makarov, M.P. Malyavkin, E.A. Ryabov, E.G. Silkis and V.D. Titov, Appl. Phys. 22 (1980) 101;
(b) V.N. Bagratashvili, Yu.G. Vainer, V.S. Doljikov, V.S. Letokhov, A.A. Makarov, M.P. Malyavkin, E.A. Ryabov and E.G. Silkis, Opt. Letters 6 (1981) 148;
(c) V.N. Bagratashvili, V.S. Doljikov, V.S. Letokhov, A.A. Makarov, L.P. Malyavkin, E.A. Ryabov, E.G. Silkis, and Yu.G. Vainer, Opt. Commun. 38 (1981) 31.
[7] R.V. Ambartzumian, G.N. Makarov and A.A. Puretzky, Opt. Commun. 34 (1980) 81.
[8] (a) S.L. McCall and E.L. Hahn, Phys. Rev. Letters 18 (1967) 908;
(b) M.O. Bulanin and I.A. Popov, Soviet Tech. Phys. Letters 4 (1978) 557;
(c) P. Bernard, P. Galarneau and S.L. Chin, Opt. Letters 6 (1981) 139.
[9] P.A. Schulz, Aa.S. Sudbo, E.R. Grant, Y.R. Shen and Y.T. Lee, J. Chem. Phys. 72 (1980) 4985.
[10] D.M. Brenner, J. Chem. Phys. 74 (1981) 2293.
[11] T.E. Gough, R.E. Miller and G. Scoles, Appl. Phys. Letters 30 (1977) 338.
[12] T.E. Gough, R.E. Miller and G. Scoles, J. Mol. Spectry. 72 (1978) 124.
[13] T.E. Gough, R.E. Miller and G. Scoles, J. Chem. Phys. 69 (1978) 1558; J. Phys. Chem. 85 (1981) 4041.
[14] S. Avrillier, J.M. Raimond, Ch. J. Bordè, D. Bassi and G. Scoles, Opt. Commun. 39 (1981) 311.
[15] D. Bassi, A. Boschetti, S. Marchetti, G. Scoles and M. Zen, J. Chem. Phys. 74 (1981) 2221.
[16] V.N. Bagratashvili, I.N. Knyazev, V.S. Letokhov and V.V. Lobko, Opt. Commun. 18 (1976) 525.
[17] G. Gallinaro, G. Roba and R. Tatarek, J. Phys. E11 (1978) 628.
[18] D. Bassi, A. Boschetti, M. Scotoni and M. Zen, Appl. Phys. B26 (1981) 99.
[19] J. Geraedts, S. Setiadi, S. Stolte and J. Reuss, Chem. Phys. Letters 78 (1981) 277;
J. Geraedts, S. Stolte and J. Reuss, Z. Physik. A304 (1982) 167.
[20] J.B. Anderson, R.P. Andres and J.B. Fenn, Advan. At. Mol. Phys. 1 (1965) 345; Advan. Chem. Phys. 10 (1966) 275.
[21] J.I. Steinfeld, I. Burak, D.G. Sutton and A.V. Nowak, J. Chem. Phys. 52 (1970) 5421.
[22] G. Luijks, S. Stolte and J. Reuss, Chem. Phys. 62 (1981) 217.
[23] D.R. Coulter, F.R. Grabiner, L.M. Casson, G.W. Flynn and R.B. Bernstein, J. Chem. Phys. 73 (1980) 281.
[24] P.K. Sharma, W.S. Young, W.E. Rodgers and E.L. Knuth, J. Chem. Phys. 62 (1975) 341.
[25] A. Porter and A.F. Grosser, Mol. Phys. 38 (1979) 611.
[26] S.S. Fisher, Phys. Fluids 22 (1979) 1261.
[27] H. Ashkenas and F.S. Sherman, in: Rarefied gas dynamics, Vol. 2, ed. J.H. de Leeuw (Academic Press, New York, 1966) p. 84.
[28] P. Huber-Wälchli and J.W. Nibler, J. Chem. Phys. 76 (1982) 273.
[29] C. Brodbeck, I. Rossi, H. Strapelias and J.P. Bouanich, Chem. Phys. 54 (1980) 1.